

Fair Class-Incremental Learning using Sample Weighting

Jaeyoung Park*

Korea Advanced Institute of Science
and Technology
Daejeon, Republic of Korea
jypark@kaist.ac.kr

Minsu Kim*

Korea Advanced Institute of Science
and Technology
Daejeon, Republic of Korea
ms716@kaist.ac.kr

Steven Euijong Whang[†]

Korea Advanced Institute of Science
and Technology
Daejeon, Republic of Korea
swhang@kaist.ac.kr

Abstract

Model fairness is becoming important in class-incremental learning for Trustworthy AI. While accuracy has been a central focus in class-incremental learning, fairness has been relatively understudied. However, naïvely using all the samples of the current task for training results in *unfair catastrophic forgetting* for certain sensitive groups including classes. We theoretically analyze that forgetting occurs if the average gradient vector of the current task data is in an “opposite direction” compared to the average gradient vector of a sensitive group, which means their inner products are negative. We then propose a *fair class-incremental learning* framework that adjusts the training weights of current task samples to change the direction of the average gradient vector and thus reduce the forgetting of underperforming groups and achieve fairness. For various group fairness measures, we formulate optimization problems to minimize the overall losses of sensitive groups while minimizing the disparities among them. We also show the problems can be solved with linear programming and propose an efficient Fairness-aware Sample Weighting (FSW) algorithm. Experiments show that FSW achieves better accuracy-fairness tradeoff results than state-of-the-art approaches on real datasets. The source code is released at <https://github.com/jyparkkr/FSW>.

CCS Concepts

• Computing methodologies → Machine learning.

Keywords

trustworthy ai, model fairness, continual learning, class-incremental learning

Full version. This document contains additional results and appendices omitted from the KDD '26 version due to space limits. The Version of Record will appear in the ACM Digital Library. DOI: <https://doi.org/10.1145/3770854.3780167>

1 Introduction

Trustworthy AI is becoming critical in various continual learning applications including autonomous vehicles, personalized recommendations, healthcare monitoring, and more [45, 56]. Improving both model fairness and accuracy is crucial, as unfair predictions can significantly compromise trust and safety, particularly in human-centered automated systems, especially as observed frequently in the context of continual learning. In this paper, we focus on class-incremental learning, where the objective is to incrementally learn new classes as they appear.

*Equal contribution.

[†]Corresponding author.

The main challenge of class-incremental learning is to learn new classes of data, while not forgetting previously-learned classes [12, 53]. If we simply fine-tune the model on the new classes, the model will gradually forget about the previously-learned classes. This phenomenon called catastrophic forgetting [51, 63, 70] may easily occur in real-world scenarios where the model needs to continuously learn new classes. Therefore, we need to have a balance between learning new information and retaining previously-learned knowledge, which is called the stability-plasticity dilemma [1, 49, 65].

In this paper, we solve the problem of *fair class-incremental learning* where the goal is to satisfy various notions of fairness among sensitive groups including classes in addition to classifying accurately. In continual learning, unfair forgetting may occur if the current task data has similar characteristics to previous data, but belongs to different sensitive groups including classes, which negatively affects the performance on the previous data during training. Despite the importance of the problem, the existing research [21, 81] is still nascent and has limitations in terms of technique or scope (see Sec. 2). In comparison, we support fairness more generally in class-incremental learning by satisfying various notions of group fairness for sensitive groups including classes.

We demonstrate how unfair forgetting can occur on a synthetic dataset with two attributes (x_1, x_2) , and one true label y as shown in Fig. 1a. We sample data for each class from three normal distributions: $(x_1, x_2)|y = 0 \sim \mathcal{N}([-2; -2], [1; 1])$, $(x_1, x_2)|y = 1 \sim \mathcal{N}([2; 4], [1; 1])$, and $(x_1, x_2)|y = 2 \sim \mathcal{N}([4; 2], [1; 1])$. To simulate class-incremental learning, we introduce data for Class 0 (blue) and Class 1 (orange) in Task 1, followed by Class 2 (green) data in Task 2, where Class 2’s data is similar to Class 1’s data. We observe that this setting frequently occurs in real datasets, where different classes of data exhibit similar features or characteristics, as shown in Sec. B.1. We assume a data replay setting in which only a limited amount of data from Classes 0 and 1 is stored and jointly used during training on Class 2. After completing training on Task 1, we observe how the model’s accuracy on the three classes changes during Task 2 training in Fig. 1b. As the accuracy on Class 2 improves, there is a catastrophic forgetting of Class 1 only, which leads to unfairness.

Beyond the label, unfairness can also arise when forgetting occurs among groups defined by both label y and a sensitive attribute z such as age, gender, or race. For instance, we can consider Class 0 as $(y = 0, z = 0)$, Class 1 as $(y = 0, z = 1)$, and Class 2 as $(y = 1, z = 1)$. Introducing Class 2 in Task 2 can lead to an accuracy drop on Class 1 ($z = 1$), while Class 0 ($z = 0$) remains unaffected. Likewise, unfairness can arise when groups are defined by both class labels and sensitive attributes.

To analytically understand the unfair forgetting, we project the average gradient vector for each class data on a 2-dimensional space in Fig. 1c. Here g_0 , g_1 , and g_2 represent the average gradient

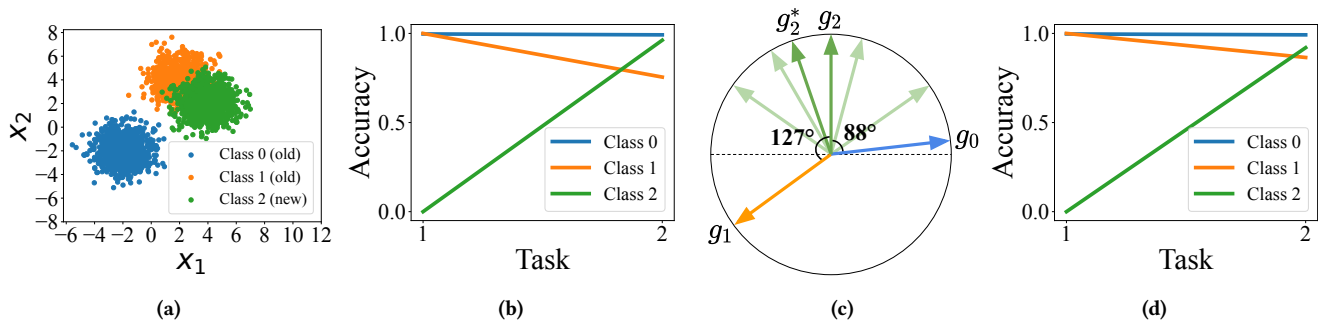


Figure 1: (a) A synthetic dataset for class-incremental learning. (b) Training on Class 2 results in unfair forgetting on Class 1 only. (c) The average gradient vector of Class 2, g_2 , is more than 90° apart from Class 1’s g_1 , which means the model is being trained in an opposite direction. Our method adjusts g_2 to g_2^* through sample weighting to be closer to g_1 , but not too far from the original g_2 . (d) As a result, the unfair forgetting is mitigated while minimally sacrificing accuracy for Class 2.

vectors of the samples of Classes 0, 1, and 2, respectively. We observe that g_2 is 127° apart from g_1 , but 88° from g_0 , which means that the inner products $\langle g_2, g_1 \rangle$ and $\langle g_2, g_0 \rangle$ are negative and close to 0, respectively. In Sec. 3.1, we theoretically show that a negative inner product between average gradient vectors of current and previous data results in higher loss for the previous data as the model is being updated in an opposite direction and identify a sufficient condition for unfair forgetting. As a result, Class 1’s accuracy decreases, while Class 0’s accuracy remains stable.

Our solution to mitigate unfair forgetting is to adjust the average gradient vector of the current task data by weighting its samples. The light-green vectors in Fig. 1c are the gradient vectors of individual samples from Class 2, and by weighting them we can adjust g_2 to g_2^* to make the inner product with g_1 less negative. At the same time, we do not want g_2^* to be too different from g_2 and lose accuracy. In Sec. 3.2, we formalize this idea using the weighted average gradient vector of the current task data. We then optimize the sample weights such that unfair forgetting and accuracy reduction over sensitive groups including classes are both minimized. We show this optimization can be solved with linear programming and propose our efficient Fairness-aware Sample Weighting (FSW) algorithm. Fig. 1d shows how using FSW mitigates the unfair forgetting between Classes 0 and 1 without harming Class 2’s accuracy much. Our framework supports the group fairness measures equal error rate [83], equalized odds [38], and demographic parity [33] and can be potentially extended to other measures.

In our experiments, we show that FSW achieves better fairness and competitive accuracy compared to state-of-the-art baselines on various image, text, and tabular datasets. The benefits come from assigning different training weights to the current task samples with accuracy and fairness in mind.

Summary of Contributions: (1) We theoretically analyze how unfair catastrophic forgetting can occur in class-incremental learning; (2) We formulate optimization problems for mitigating the unfairness for various group fairness measures and propose an efficient fairness-aware sample weighting algorithm, FSW; (3) We demonstrate how FSW outperforms state-of-the-art baselines in terms of fairness with comparable accuracy on various datasets.

2 Related Work

Class-incremental learning is a challenging type of continual learning where a model continuously learns new tasks, each composed of new disjoint classes, and the goal is to minimize catastrophic forgetting [60, 61]. Data replay techniques [20, 58, 73] store a small portion of previous data in a buffer to utilize for training and are widely used with other techniques (see more details in Sec. C). There are also more advanced gradient-based sample selection techniques like GSS [4] and OCS [92] that manage buffer data to have samples with diverse and representative gradient vectors. All these works do not consider fairness and simply assume that the entire incoming data is used for model training, which may result in unfair forgetting as we show in our experiments.

Model fairness research mitigates bias by ensuring that a model’s performance is equitable across different sensitive groups, thereby preventing discrimination based on race, gender, age, or other sensitive attributes [64] (see more details in Sec. C). However, most of these techniques assume that the training data is given all at once, which may not be realistic. There are techniques for fairness-aware active learning [5, 68, 80], in which the training data evolves with the acquisition of samples. However, these techniques store all labeled data and use them for training, which is impractical in continual learning settings.

A recent study addresses model fairness in class-incremental learning, where models may suffer from imbalanced forgetting of previously learned sensitive groups including classes, leading to unfairness across different groups [21, 39, 81, 88] (see more details in Sec. C). FairRL [21] supports group fairness metrics like demographic parity for continual learning, but proposes a representation learning method that does not directly optimize the given fairness measure and thus has limitations in improving fairness as we show in experiments. FairCL [81] also addresses fairness in a continual learning setup, but only focuses on resolving the imbalanced class distribution based on the number of pixels of each class in an image, and is specific to semantic segmentation tasks. In comparison, we can mitigate bias from both data imbalance and intrinsic or acquired characteristics within the data by satisfying multiple notions of group fairness for sensitive groups including classes.

3 Framework

In this section, we first theoretically analyze unfair forgetting using gradient vectors of sensitive groups and the current task data. Next, we propose a sample weighting algorithm to mitigate unfairness by adjusting the average gradient vector of the current task data.

Notations. In class-incremental learning, a model incrementally learns new current task data along with previous buffer data using data replay. Suppose we train a model to incrementally learn L tasks $\{T_1, T_2, \dots, T_L\}$ over time, and there are N classes in each task with no overlapping classes between different tasks. After learning the l^{th} task T_l , we would like the model to remember all $(l-1) \cdot N$ previous task classes and an additional N current task classes. We assume the buffer has a fixed size of M samples. For L tasks, we allocate $m = M/L$ samples of buffer data per task. If each task consists of N classes, then we allocate $m/N = M/(L \cdot N)$ samples of buffer data per class [18, 19, 66]. Each task $T_l = \{d_i = (X_i, y_i)\}$ is composed of feature-label pairs. We also use $\mathcal{M}_l = \{d_j = (X_j, y_j)\}_{j=1}^m$ to represent the buffer data for each previous l^{th} task T_l . We assume the buffer data per task is small, i.e., $m \ll |T_l|$ [20].

When defining fairness for class-incremental learning, we utilize sensitive groups including classes. According to the fairness literature, sensitive groups are divided by sensitive attributes like gender and race (e.g., Male and Female). Similarly, the classes can also be viewed as sensitive groups, where the class label serves as the sensitive attribute. To support either case in a class-incremental setting, we use the following unifying notations: (1) if the sensitive groups are classes, then they form the set $G_y = \{(X, y) \in \mathcal{D} : y = y, y \in \mathbb{Y}\}$ where \mathcal{D} is a dataset, y is a class attribute, and \mathbb{Y} is the set of y ; (2) if we are using sensitive attributes beyond classes, we can further divide the classes into the set $G_{y,z} = \{(X, y, z) \in \mathcal{D} : y = y, z = z, y \in \mathbb{Y}, z \in \mathbb{Z}\}$ where z is a sensitive attribute and \mathbb{Z} is the set of z . See Sec. A.1 for a summary of notations used.

3.1 Unfair Forgetting

We take inspiration from GEM [58], which theoretically analyzes catastrophic forgetting by utilizing the angle between gradient vectors of data. If the inner products of gradient vectors for previous tasks and the current task are negative (i.e., $90^\circ < \text{angle} \leq 180^\circ$), the loss of previous tasks increases after learning the current task. Catastrophic forgetting thus occurs when the gradient vectors of different tasks point in opposite directions. Intuitively, the opposite gradient vectors update the model parameters in conflicting directions, leading to forgetting while learning.

Using the notion of catastrophic forgetting, we propose theoretical results for unfair forgetting:

LEMMA 3.1. *Denote G as a sensitive group containing features X and true labels y . Also, denote f_θ^{l-1} as a previous model and f_θ as the updated model after training on the current task T_l . Let ℓ be any differentiable loss function (e.g., cross-entropy loss), and η be a learning rate. Then, the loss of the sensitive group of data after training with a current task sample $d_i \in T_l$ is approximated as:*

$$\tilde{\ell}(f_\theta, G) = \ell(f_\theta^{l-1}, G) - \eta \nabla_\theta \ell(f_\theta^{l-1}, G)^\top \nabla_\theta \ell(f_\theta^{l-1}, d_i), \quad (1)$$

where $\tilde{\ell}(f_\theta, G)$ is the approximated average loss between model predictions $f_\theta(X)$ and true labels y , whereas $\ell(f_\theta^{l-1}, G)$ is the exact average

loss, $\nabla_\theta \ell(f_\theta^{l-1}, G)$ is the average gradient vector for the samples in the group G , and $\nabla_\theta \ell(f_\theta^{l-1}, d_i)$ is the gradient vector for a sample d_i , each with respect to the previous model f_θ^{l-1} .

The proof is in Sec. A.2. We employ first-order Taylor series approximation for the proof, which is widely used in the continual learning literature, by assuming that the loss function is locally linear in small optimization steps and considering the first-order term as the cause of catastrophic forgetting [4, 55, 58]. We empirically find that the approximation error is large when a new task begins because new samples with unseen classes are introduced. However, the error gradually becomes quite small as the number of epochs increases while training a model for the task, as in Sec. B.2. Additionally, while higher-order terms can be included in principle, doing so makes the optimization non-convex and NP-hard. A detailed proof is provided in Sec. A.3.

To define fairness in class-incremental learning with the approximated loss, we adopt the definition of approximate fairness that considers a model to be fair if it has approximately the same loss on the positive class, independent of the group membership [30]. In this paper, we compute fairness measures based on the disparity between approximated cross-entropy losses, which are derived from Lemma 3.1 using gradients. The following proposition shows how using the cross-entropy loss disparity can effectively approximate common group fairness metrics such as equalized odds and demographic parity. We choose cross-entropy loss specifically because it is widely validated as a strong proxy for fairness disparity metrics, though our method is robust to alternative loss choices (see Sec. A.4 and B.14 for more justification of the loss function and an alternative, respectively).

PROPOSITION 3.2. *(From [75, 76, 78]) Using the cross-entropy loss disparity to measure fairness is empirically verified to provide reasonable proxies for common group fairness metrics.*

Based on Lemma 3.1 and Proposition 3.2, Theorem 3.3 provides a sufficient condition for unfair forgetting. Intuitively, if a sample's gradient opposes only the underperforming group's average gradient, the training amplifies unfairness between the two groups.

THEOREM 3.3. *Let ℓ be the cross-entropy loss and G_1 and G_2 the overperforming and underperforming sensitive groups of data, respectively. Also let d_i be a training sample that satisfy the following conditions: $\ell(f_\theta^{l-1}, G_1) < \ell(f_\theta^{l-1}, G_2)$ while $\nabla_\theta \ell(f_\theta^{l-1}, G_1)^\top \nabla_\theta \ell(f_\theta^{l-1}, d_i) > 0$ and $\nabla_\theta \ell(f_\theta^{l-1}, G_2)^\top \nabla_\theta \ell(f_\theta^{l-1}, d_i) < 0$. Then $|\tilde{\ell}(f_\theta, G_1) - \tilde{\ell}(f_\theta, G_2)| > |\ell(f_\theta^{l-1}, G_1) - \ell(f_\theta^{l-1}, G_2)|$.*

The proof is in Sec. A.2. The result shows that the loss disparity between the two groups could become larger after training on the current task sample, which leads to worse fairness. This theorem can be extended to when we have a set of current task samples $T_l = \{d_i = (X_i, y_i)\}$ where we can replace $\nabla_\theta \ell(f_\theta^{l-1}, d_i)$ with $\frac{1}{|T_l|} \sum_{d_i \in T_l} \nabla_\theta \ell(f_\theta^{l-1}, d_i)$. If the average gradient vector of the current task data satisfies the derived sufficient condition, training with all of the current task samples using equal weights could thus result in unfair catastrophic forgetting.

3.2 Sample Weighting for Unfairness Mitigation

To mitigate unfairness, we propose sample weighting to suppress samples that harm fairness and promote samples that help. Given training weights $\mathbf{w}_l \in [0, 1]^{|T_l|}$ for the samples in the current task data, the approximated loss of a group G after training is:

$$\tilde{\ell}(f_\theta, G) = \ell(f_\theta^{l-1}, G) - \eta \nabla_\theta \ell(f_\theta^{l-1}, G)^\top \left(\frac{1}{|T_l|} \sum_{d_i \in T_l} \mathbf{w}_l^i \nabla_\theta \ell(f_\theta^{l-1}, d_i) \right),$$

where \mathbf{w}_l^i is a training weight for the current task sample d_i . We then formulate an optimization problem to find the weights such that both loss and unfairness are minimized. Here we define \mathbb{Y} as the set of all classes and \mathbb{Y}_c as the set of classes in the current task. We represent accuracy as the average loss over the current task data and minimize the cost function $\mathcal{L}_{acc} = \tilde{\ell}(f_\theta, G_{\mathbb{Y}_c}) = \frac{1}{|\mathbb{Y}_c|} \sum_{y \in \mathbb{Y}_c} \tilde{\ell}(f_\theta, G_y) = \frac{1}{|\mathbb{Y}_c| |\mathbb{Z}|} \sum_{y \in \mathbb{Y}_c, z \in \mathbb{Z}} \tilde{\ell}(f_\theta, G_{y,z})$. For fairness, the cost function \mathcal{L}_{fair} depends on the group fairness measure as we explain below. We then minimize $\mathcal{L}_{fair} + \lambda \mathcal{L}_{acc}$ where λ is a hyperparameter that balances fairness and accuracy.

Equal Error Rate (EER). This measure [83] is defined as $\Pr(\hat{y} \neq y_1 | y = y_1) = \Pr(\hat{y} \neq y_2 | y = y_2)$ for $y_1, y_2 \in \mathbb{Y}$, where \hat{y} is the predicted class, and y is the true class. We define the cost function for EER as the average absolute deviation of the class loss, consistent with the definition of group fairness metrics: $\mathcal{L}_{EER} = \frac{1}{|\mathbb{Y}|} \sum_{y \in \mathbb{Y}} |\tilde{\ell}(f_\theta, G_y) - \tilde{\ell}(f_\theta, G_{\mathbb{Y}})|$. The entire optimization problem is:

$$\begin{aligned} \min_{\mathbf{w}_l} \frac{1}{|\mathbb{Y}|} \sum_{y \in \mathbb{Y}} |\tilde{\ell}(f_\theta, G_y) - \tilde{\ell}(f_\theta, G_{\mathbb{Y}})| + \lambda \frac{1}{|\mathbb{Y}_c|} \sum_{y \in \mathbb{Y}_c} \tilde{\ell}(f_\theta, G_y), \\ \text{where } \tilde{\ell}(f_\theta, G_y) = \ell(f_\theta^{l-1}, G_y) \\ - \eta \nabla_\theta \ell(f_\theta^{l-1}, G_y)^\top \left(\frac{1}{|T_l|} \sum_{d_i \in T_l} \mathbf{w}_l^i \nabla_\theta \ell(f_\theta^{l-1}, d_i) \right). \end{aligned} \quad (2)$$

Equalized Odds (EO). This measure [38] is satisfied when sensitive groups have the same accuracy, i.e., $\Pr(\hat{y} = y | y = y, z = z_1) = \Pr(\hat{y} = y | y = y, z = z_2)$ for $y \in \mathbb{Y}$ and $z_1, z_2 \in \mathbb{Z}$. We design the cost function for EO as $\mathcal{L}_{EO} = \frac{1}{|\mathbb{Y}| |\mathbb{Z}|} \sum_{y \in \mathbb{Y}, z \in \mathbb{Z}} |\tilde{\ell}(f_\theta, G_{y,z}) - \tilde{\ell}(f_\theta, G_y)|$, and the entire optimization problem is:

$$\begin{aligned} \min_{\mathbf{w}_l} \frac{1}{|\mathbb{Y}| |\mathbb{Z}|} \sum_{y \in \mathbb{Y}, z \in \mathbb{Z}} |\tilde{\ell}(f_\theta, G_{y,z}) - \tilde{\ell}(f_\theta, G_y)| \\ + \lambda \frac{1}{|\mathbb{Y}_c| |\mathbb{Z}|} \sum_{y \in \mathbb{Y}_c, z \in \mathbb{Z}} \tilde{\ell}(f_\theta, G_{y,z}), \\ \text{where } \tilde{\ell}(f_\theta, G_{y,z}) = \ell(f_\theta^{l-1}, G_{y,z}) \\ - \eta \nabla_\theta \ell(f_\theta^{l-1}, G_{y,z})^\top \left(\frac{1}{|T_l|} \sum_{d_i \in T_l} \mathbf{w}_l^i \nabla_\theta \ell(f_\theta^{l-1}, d_i) \right). \end{aligned} \quad (3)$$

Demographic Parity (DP). This measure [33] is satisfied by minimizing the difference in positive prediction rates between sensitive groups. Here, we extend the notion of demographic parity to the multi-class setting [3, 28], i.e., $\Pr(\hat{y} = y | z = z_1) = \Pr(\hat{y} = y | z = z_2)$ for $y \in \mathbb{Y}$ and $z_1, z_2 \in \mathbb{Z}$. In the binary setting of $\mathbb{Y} = \mathbb{Z} = \{0, 1\}$, a sufficient condition for demographic parity is suggested using the loss multiplied by the ratios of sensitive groups [75]. By extending to multi-class, we derive a sufficient condition as follows: $\frac{m_{y,z_1}}{m_{*,z_1}} \ell(f_\theta, G_{y,z_1}) = \frac{m_{y,z_2}}{m_{*,z_2}} \ell(f_\theta, G_{y,z_2})$ where

Algorithm 1 Fair Class-Incremental Learning

Input: Current task data T_l , previous buffer data $\mathcal{M} = \{\mathcal{M}_1, \dots, \mathcal{M}_{l-1}\}$, previous model f_θ^{l-1} , loss function ℓ , learning rate η , hyperparameters $\{\alpha, \lambda, \tau\}$, and fairness measure F .

- 1: **for** each epoch **do**
- 2: $\mathbf{w}_l^* \leftarrow \text{FSW}(T_l, \mathcal{M}, f_\theta^{l-1}, \ell, \alpha, \lambda, F)$
- 3: $g_{\text{curr}} \leftarrow \frac{1}{|T_l|} \sum_{d_i \in T_l} \mathbf{w}_l^{*i} \nabla_\theta \ell(f_\theta^{l-1}, d_i)$
- 4: $g_{\text{prev}} \leftarrow \nabla_\theta \ell(f_\theta^{l-1}, \mathcal{M})$
- 5: $\theta \leftarrow \theta - \eta (g_{\text{curr}} + \tau g_{\text{prev}})$
- 6: $\mathcal{M}_l \leftarrow \text{Buffer Sample Selection}(T_l)$
- 7: $\mathcal{M} \leftarrow \mathcal{M} \cup \mathcal{M}_l$

$m_{y,z} := |\{i : y_i = y, z_i = z\}|$ and $m_{*,z} := |\{i : z_i = z\}|$. The proof is in Sec. A.5. Let us define $\ell'(f_\theta, G_{y,z}) = \frac{m_{y,z}}{m_{*,z}} \ell(f_\theta, G_{y,z})$ and $\ell'(f_\theta, G_y) = \frac{1}{|\mathbb{Z}|} \sum_{n=1}^{|\mathbb{Z}|} \frac{m_{y,z_n}}{m_{*,z_n}} \ell(f_\theta, G_{y,z_n})$. We then define the cost function for DP as $\mathcal{L}_{DP} = \frac{1}{|\mathbb{Y}| |\mathbb{Z}|} \sum_{y \in \mathbb{Y}, z \in \mathbb{Z}} |\tilde{\ell}'(f_\theta, G_{y,z}) - \tilde{\ell}'(f_\theta, G_y)|$. The entire optimization problem is:

$$\begin{aligned} \min_{\mathbf{w}_l} \frac{1}{|\mathbb{Y}| |\mathbb{Z}|} \sum_{y \in \mathbb{Y}, z \in \mathbb{Z}} |\tilde{\ell}'(f_\theta, G_{y,z}) - \tilde{\ell}'(f_\theta, G_y)| \\ + \lambda \frac{1}{|\mathbb{Y}_c| |\mathbb{Z}|} \sum_{y \in \mathbb{Y}_c, z \in \mathbb{Z}} \tilde{\ell}'(f_\theta, G_{y,z}), \end{aligned} \quad (4)$$

where $\tilde{\ell}'(f_\theta, G_{y,z}) = \ell(f_\theta^{l-1}, G_{y,z})$

$$- \eta \nabla_\theta \ell(f_\theta^{l-1}, G_{y,z})^\top \left(\frac{1}{|T_l|} \sum_{d_i \in T_l} \mathbf{w}_l^i \nabla_\theta \ell(f_\theta^{l-1}, d_i) \right).$$

To find the optimal sample weights for the current task data considering both model accuracy and fairness, we first transform the defined optimization problems of Eqs. 2, 3, and 4 into the form of linear programming (LP) problems.

THEOREM 3.4. *The fairness-aware optimization problems (Eqs. 2, 3, and 4) can be formulated as linear programming (LP) problems.*

The loss of each group can be approximated as a linear function, as described in Lemma 3.1. This result implies that the optimization problems, consisting of the loss of each group, can likewise be formulated as LP problems. The proof is in Sec. A.6. We solve the LP problems using linear optimization solvers (e.g., CPLEX [26]). As we add the average loss of the current task data in Eqs. 2, 3, and 4 as a regularization term, the optimal sample weights do not indicate a severely shifted distribution.

3.3 Algorithm

We describe the overall process of fair class-incremental learning in Alg. 1. For the recently arrived current task data, we first perform our fairness-aware sample weighting (FSW) to assign training weights that can help learn new knowledge of the current task while retaining accurate and fair memories of previous tasks (Step 2). Next, we train the model using the current task data with its corresponding weights and stored buffer data of previous tasks (Steps 3–5), where η is a learning rate, and τ is a hyperparameter to balance between them during training. The sample weights are computed once at the beginning of each epoch, and they are applied to all batches for computational efficiency [47, 48]. This procedure

Algorithm 2 Fairness-aware Sample Weighting (FSW)

Input: Current task data $T_l = \{\dots, d_i, \dots\}$, previous buffer data, $\mathcal{M} = \bigcup_{y \in \mathcal{Y}, z \in \mathcal{Z}} G_{y,z}$, previous model f_{θ}^{l-1} , loss ℓ , hyperparameters $\{\alpha, \lambda\}$, and fairness measure F .

Output: Optimal training weights w_i^* for current task data

- 1: $\ell_G \leftarrow [\ell(f_{\theta}^{l-1}, G_{1,1}), \dots, \ell(f_{\theta}^{l-1}, G_{|\mathcal{Y}|,|\mathcal{Z}|})]$
- 2: $g_G \leftarrow [\nabla_{\theta} \ell(f_{\theta}^{l-1}, G_{1,1}), \dots, \nabla_{\theta} \ell(f_{\theta}^{l-1}, G_{|\mathcal{Y}|,|\mathcal{Z}|})]$
- 3: $g_d \leftarrow [\dots, \nabla_{\theta} \ell(f_{\theta}^{l-1}, d_i), \dots]$
- 4: **switch** F **do**
- 5: **case** EER: $w_i^* \leftarrow$ Solve Eq. 2
- 6: **case** EO: $w_i^* \leftarrow$ Solve Eq. 3
- 7: **case** DP: $w_i^* \leftarrow$ Solve Eq. 4
- 8: **return** w_i^*

is repeated until the model converges (Steps 1–5). Before moving on to the next task, we employ buffer sample selection to store a small data subset for the current task (Steps 6–7). Buffer sample selection can also be done with consideration for fairness, but our experimental observations indicate that selecting representative and diverse samples for the buffer, as previous studies have shown, results in better accuracy and fairness. We thus employ a simple random sampling technique for the buffer sample selection in our framework (see Sec. B.15 for more details).

Alg. 2 shows the fairness-aware sample weighting (FSW) algorithm for the current task data. We first divide both the previous buffer data and the current task data into groups based on each class and sensitive attribute. Next, we compute the average loss and gradient vectors for each group (Steps 1–2), and individual gradient vectors for the current task data (Step 3). To compute gradient vectors, we use the last layer approximation, which only considers the gradients of the model’s last layer, that is efficient and known to be reasonable [9, 44, 47, 48, 50, 67] (see Sec. B.16 for details). We then solve linear programming to find the optimal sample weights for a user-defined target fairness measure such as EER (Step 5), EO (Step 6), and DP (Step 7). Since the gradient norm of the current task data is significantly larger than that of the buffer data, we utilize normalized gradients to update the loss of each group and replace the learning rate η with a hyperparameter α in the equations. Finally, we return the current task’s sample weights for training (Step 8).

Training with FSW theoretically guarantees model convergence under the assumptions that the training loss is Lipschitz continuous and strongly convex, and that a proper learning rate is used [16, 47, 59]. The computational complexity of FSW is quadratic to the number of current task samples, as CPLEX, which uses simplex-based algorithms, typically exhibits quadratic complexity with respect to the number of variables when solving LP problems in practice [13]. Our empirical results show that for about twelve thousand current task samples, the time to solve an LP problem is a few seconds, which leads to a few minutes of overall runtime for MNIST datasets (see Sec. B.3 for details). Since we focus on continual offline training of large batches or separate tasks, rather than online learning, the overhead is manageable enough to deploy updated models in real-world applications. If the task size becomes too large, clustering similar samples and assigning weights to the clusters, rather than samples, could be a solution to reduce the computational overhead.

Table 1: Experimental settings for the five datasets.

Dataset	Size	#Features	#Classes	#Tasks
MNIST	60K	28×28	10	5
FMNIST	60K	28×28	10	5
Biased MNIST	60K	3×28×28	10	5
DRUG	1.3K	12	6	3
BiasBios	253K	128×768	25	5

4 Experiments

In this section, we construct experiments on FSW and address the following research questions: **RQ1** How well can FSW mitigate the unfair forgetting that occurs in class-incremental learning with better accuracy-fairness tradeoff? **RQ2** How does FSW weight the samples? **RQ3** Can FSW be further integrated with fair post-processing techniques?

4.1 Experiment Settings

4.1.1 Metrics. We follow the prior fair continual learning literature to evaluate accuracy and fairness [21, 81].

Average Accuracy. We denote $A_l = \frac{1}{T} \sum_{t=1}^l a_{l,t}$ as the accuracy at the l^{th} task, where $a_{l,t}$ is the accuracy of the l^{th} task after learning the t^{th} task. We average A_l over all tasks to obtain the final average accuracy, $\bar{A}_l = \frac{1}{L} \sum_{l=1}^L A_l$ where L is the total number of tasks.

Average Fairness. We measure fairness for each task and then average these values to obtain the overall fairness score. Depending on the evaluation scenario, we select one of three disparity measures. In all cases, lower disparity indicates better fairness.

(1) *EER* computes the average difference in test error rates among classes: $\frac{1}{|\mathcal{Y}|} \sum_{y \in \mathcal{Y}} |\Pr(\hat{y} \neq y | y = y) - \Pr(\hat{y} \neq y)|$. EER targets fairness in predictive quality, aiming for equitable accuracy or error across different prediction outcomes. EER is used as a target metric where a sensitive attribute (z) is not explicitly provided. This scenario includes commonly used class-incremental learning benchmarks where only the class label (y) is available. In such cases, EER serves as a practical proxy for fairness under task imbalance, focusing on equal error across classes.

On the other hand, when z is available, fairness can also be evaluated using group-based metrics like EO and DP, which use both y and z to cover broader social norms.

(2) *EO disparity* computes the average difference in accuracy among sensitive groups for all classes: $\frac{1}{|\mathcal{Y}||\mathcal{Z}|} \sum_{y \in \mathcal{Y}, z \in \mathcal{Z}} |\Pr(\hat{y} = y | y = y, z = z) - \Pr(\hat{y} = y | y = y)|$. EO is preferred when ensuring equal model performance across groups or when true/false positives are equally important.

(3) *DP disparity* computes the average difference in class prediction ratios among sensitive groups for all classes: $\frac{1}{|\mathcal{Y}||\mathcal{Z}|} \sum_{y \in \mathcal{Y}, z \in \mathcal{Z}} |\Pr(\hat{y} = y | z = z) - \Pr(\hat{y} = y)|$. DP is preferred when mitigating data bias or achieving ‘blind fairness’ by equalizing output distributions.

4.1.2 Datasets. We use a total of five datasets as shown in Table 1. We first utilize commonly used benchmarks for continual image

Table 2: Accuracy and fairness results with respect to (1) EER disparity, where class is considered the sensitive attribute for MNIST and FMNIST datasets, and (2) EO disparity, where background color and gender are the sensitive attributes for the Biased MNIST and DRUG datasets, respectively (see DP disparity and the BiasBios dataset results in Sec. B.6). We mark the best and second-best results with bold and underline, respectively, excluding the naïve methods.

Methods	MNIST		FMNIST		Biased MNIST		DRUG		BiasBios	
	Acc.	EER Disp.	Acc.	EER Disp.	Acc.	EO Disp.	Acc.	EO Disp.	Acc.	EO Disp.
Joint Training	.989 \pm .000	.003 \pm .000	.921 \pm .002	.024 \pm .002	.944 \pm .002	.108 \pm .003	.442 \pm .015	.179 \pm .052	.823 \pm .002	.076 \pm .001
Fine Tuning	.455 \pm .000	.326 \pm .000	.451 \pm .000	.325 \pm .000	.449 \pm .001	.016 \pm .002	.357 \pm .009	.125 \pm .034	.420 \pm .001	.028 \pm .002
iCaRL	.918 \pm .005	.048 \pm .003	.852\pm.002	<u>.047\pm.001</u>	.802 \pm .008	.365 \pm .021	.444\pm.025	.190 \pm .017	.829\pm.002	.084 \pm .003
WA	.911 \pm .007	.052 \pm .006	.809 \pm .005	.088 \pm .003	.916\pm.002	.140 \pm .004	.408 \pm .022	.134 \pm .029	.796 \pm .003	.076 \pm .001
CLAD	.835 \pm .016	.099 \pm .016	.782 \pm .018	.118 \pm .022	.871 \pm .012	.198 \pm .022	.410 \pm .026	.114 \pm .043	.799 \pm .003	.074 \pm .002
GSS	.889 \pm .010	.080 \pm .009	.732 \pm .021	.149 \pm .019	.809 \pm .005	.325 \pm .017	<u>.426\pm.010</u>	.167 \pm .038	<u>.808\pm.003</u>	.081 \pm .002
OCS	.929\pm.002	<u>.040\pm.003</u>	.799 \pm .008	.109 \pm .007	.824 \pm .007	.331 \pm .013	.406 \pm .024	.142 \pm .003	–	–
FaIRL	.558 \pm .060	.273 \pm .018	.531 \pm .032	.289 \pm .019	.411 \pm .012	.118\pm.011	.354 \pm .011	.060\pm.021	.400 \pm .060	.055\pm.020
FSW	<u>.925\pm.004</u>	.032\pm.005	<u>.824\pm.006</u>	.039\pm.006	<u>.909\pm.004</u>	<u>.119\pm.007</u>	.406 \pm .014	<u>.077\pm.010</u>	<u>.808\pm.002</u>	<u>.072\pm.001</u>

classification tasks, which include MNIST and Fashion-MNIST (FMNIST). Here we regard the class as the sensitive attribute and evaluate fairness with EER disparity. We also use multi-class fairness benchmark datasets that have sensitive attributes [22, 28, 72, 89]: Biased MNIST, Drug Consumption (DRUG), and BiasBios. We consider background color as the sensitive attribute for Biased MNIST, and gender for DRUG and BiasBios. We then use EO and DP disparity to evaluate fairness. We also consider using other datasets in the fairness field, but they are unsuitable for class-incremental learning experiments because either there are only two classes, or it is difficult to apply group fairness metrics (see Sec. B.4 for details).

4.1.3 Models and Hyperparameters. Following the experimental setups of [19, 66], we use a two-layer MLP with each 256 neurons for the MNIST, FMNIST, Biased MNIST, and DRUG datasets. For the BiasBios dataset, we use a pre-trained BERT language model [29]. We employ single-head evaluation where a final layer of the model is shared for all tasks [17, 31]. To solve the fairness-aware optimization problems and find optimal sample weights, we use CPLEX, a high-performance optimization solver developed by IBM that specializes in solving linear programming (LP). See Sec. B.17 for experiments comparing CPLEX with another LP solver, HiGHS [40]. For our buffer storage, we store 32 samples per sensitive group for all experiments. For the hyperparameters α , λ , and τ used in our algorithms, we perform cross-validation with a sequential grid search to find their optimal parameters. Model details and hyperparameter set are provided in Sec. B.5.

4.1.4 Baselines. Following prior work [4, 92], all baselines are continual learning methods, as other approaches do not fit this scenario. We compare FSW with algorithms from four categories:

Naïve methods. *Joint Training* assumes access to all the data from previous classes for training, thereby serving as an upper bound in terms of performance; *Fine Tuning* trains a model only on data from new classes, without access to previous data, and thus serves as a lower bound.

State-of-the-art methods. *iCaRL* [73] performs herding-based buffer selection and representation learning using knowledge distillation loss; *WA* [95] is a model rectification method designed to correct the bias in the model’s final fully-connected layer. *WA* uses weight aligning to equalize the norms of the weight vectors over classes; *CLAD* [88] is a representation learning method that disentangles the representation interference between old and new classes.

Sample selection methods. *GSS* [4] selects a buffer with diverse gradients of samples; *OCS* [92] uses gradient-based similarity, diversity, and affinity scores to rank and select samples for both current and buffer data in a unified manner.

Fairness-aware methods. *FaIRL* [21] performs fair representation learning by controlling the rate-distortion function.

Our choice of baselines was driven by practical considerations of computational cost and spatial complexity. For instance, while *L2P* [85] achieves strong performance, it leverages a pretrained vision transformer that already embeds extensive prior information, making it less directly comparable to FSW. Similarly, *DER* [90] trains a separate feature extractor for each task, which incurs additional storage overhead and complexity. In contrast, the baselines like *iCaRL* and *WA* are widely recognized as strong and representative baselines in many studies [39, 98, 99], offering a fair and practical comparison. *FairCL* [81] addresses fairness in semantic segmentation tasks arising from the imbalanced class distribution of pixels, but we consider this problem to be unrelated from ours to add the method as a baseline.

4.2 Accuracy and Fairness Results

To answer **RQ1**, we compare FSW with other baselines in terms of accuracy and corresponding fairness metrics as shown in Table 2 and Sec. B.6. The accuracy-fairness Pareto front is shown in Fig. 2 and Sec. B.7. Due to the excessive time required to run *OCS* on BiasBios, we are not able to measure the results. Detailed sequential performance results and additional analyses on varying buffer sizes are provided in Sec. B.8 and B.9, respectively.

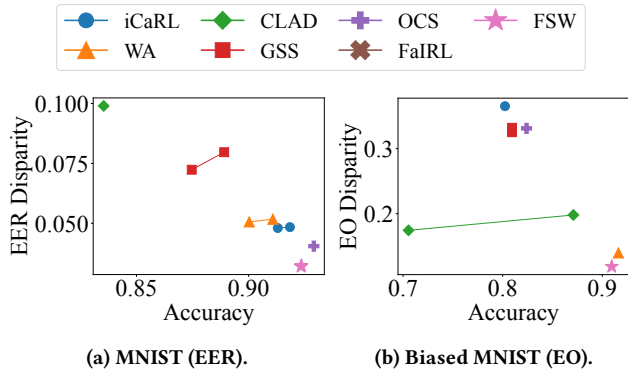


Figure 2: Tradeoff results between accuracy and fairness on the MNIST and Biased MNIST datasets. FSW positioned in the lower right corner of the graph, indicating better accuracy-fairness tradeoff results compared to other baselines.

Overall, FSW achieves better accuracy-fairness tradeoff results compared to the baselines across all the datasets. Although FSW does not achieve the best performance in accuracy, FSW shows the best fairness results among the baselines with similar accuracies (e.g., *iCaRL*, *WA*, *CLAD*, *GSS*, and *OCS*) and thus has the best accuracy-fairness tradeoff. We observe that FSW also improves model accuracy while enhancing the performance of underperforming groups for fairness.

The state-of-the-art method, *iCaRL*, generally achieves high accuracy with low EER disparity results. However, *iCaRL*'s nearest-mean-of-exemplars approach for its classification model, the predictions are significantly affected by sensitive attribute values, resulting in high disparities for EO and DP. Although *WA* also performs well, the method adjusts the model weights for the current task classes as a whole, which leads to an unfair forgetting of sensitive groups and unstable results. The closest work to FSW is *CLAD*, which disentangles the representations of new classes and a fixed proportion of conflicting old classes to mitigate imbalanced forgetting across classes. However, the proportion of conflicts may vary by task in practice, limiting *CLAD*'s ability to achieve group fairness. While the two sample selection methods *GSS* and *OCS* store diverse and representative samples in the buffer, these methods sometimes result in an imbalance in the number of buffer samples across sensitive groups. The fairness-aware method *FaIRL* leverages an adversarial debiasing framework combined with a rate-distortion function. While this method theoretically promises improved fairness, it suffers from significant accuracy degradation due to the instability of jointly training the feature encoder and discriminator.

In comparison, FSW explicitly utilizes approximated loss and fairness measures to adjust the training weights for the current task samples, which leads to better model accuracy and fairness. As shown in Fig. 2 and detailed in Sec. B.7, FSW consistently dominates the Pareto frontier, occupying the optimal bottom-right region across all evaluated tasks. These results demonstrate that FSW consistently outperforms other baselines and achieves better accuracy-fairness tradeoff.

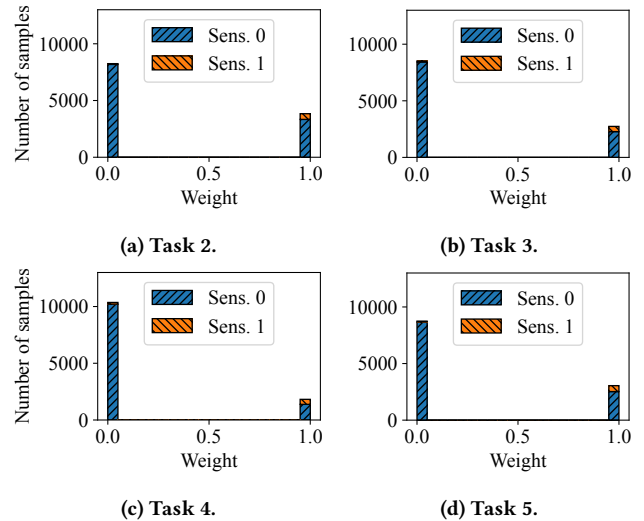


Figure 3: Distribution of sample weights for EO in sequential tasks of the Biased MNIST dataset.

Table 3: Average counts of binary (0 or 1) and non-binary (not 0 or 1) sample weights for each optimization task. Since we take averages of all tasks except the first, the sum of (# Binary) and (# Non-binary) is not necessarily an integer.

Dataset (Metric)	MNIST (EER)	FMNIST (EER)	Biased MNIST (EO)	Biased MNIST (DP)
# Binary	11830.8	11997.4	11831.9	11831.6
# Non-binary	3.0	2.6	1.9	2.1

Dataset (Metric)	Drug (EO)	Drug (DP)	BiasBios (EO)	BiasBios (DP)
# Binary	446.5	446.1	25274.7	25273.2
# Non-binary	0.0	0.4	2.0	3.5

4.3 Sample Weighting Analysis

To answer RQ2, we analyze how our FSW algorithm weights the current task samples at each task in Fig. 3 and Sec. B.10. As the acquired sample weights may change with epochs during training, we show the average weight distribution of sensitive groups over all epochs. Since FSW is not applied to the first task, where the model is trained with only the current task data, we present results starting from the second task.

The result shows that FSW assigns higher weights on average to the underperforming group (Sensitive group 1 in Fig. 3) compared to the overperforming group (Sensitive group 0 in Fig. 3). The weights are computed by considering complex forgetting relationships between sensitive groups, which differs from simply assigning higher weights to underperforming groups. Note that the acquired sample weights are mostly close to 0 or 1, which are extreme values. As optimal solutions of a linear program are obtained at the vertices of the feasible region, a convex polytope defined by

Table 4: Accuracy and fairness results on the MNIST and Biased MNIST datasets with or without FSW.

Methods	MNIST		Biased MNIST	
	Acc.	EER Disp.	Acc.	EO Disp.
W/o FSW	.912 \pm .004	.051 \pm .005	.910 \pm .003	.126 \pm .005
FSW	.925\pm.004	.032\pm.005	.909 \pm .004	.119\pm.007

Table 5: Accuracy and more fairness metrics (including EO, DP, and EER Disparity) results on the Biased MNIST dataset without FSW and FSW with respect to EO and DP disparity.

Methods	Acc.	EO Disp.	DP Disp.	EER Disp.
W/o FSW	.910\pm.003	.126 \pm .005	.009 \pm .001	.032 \pm .002
FSW (w.r.t. EO Disp.)	.909 \pm .004	.119\pm.007	.008\pm.001	.032 \pm .003
FSW (w.r.t. DP Disp.)	.904 \pm .004	.124 \pm .008	.008\pm.001	.029\pm.004

$w_l \in [0, 1]^{|T_l|}$ (as formulated in Sec. 3.2), each w coincides with its extreme values. However, there are also some values that do not lie at these boundaries (0 or 1). The number of binary (0 or 1) and non-binary (not 0 or 1) samples weights are shown in Table 3.

We also emphasize that if we limit the solution of the optimization problem to binary, which is equivalent to sample selection, the problem would transform into a mixed-integer linear programming problem, which is NP-hard and cannot be solved efficiently. We also observe that FSW assigns zero weight to a significant number of samples, reducing the training data used. This weighting approach provides an additional advantage in enabling efficient model training while retaining accuracy and fairness.

4.4 Ablation Study

To show the effectiveness of FSW on accuracy and fairness, we perform an ablation study comparing the performance of using FSW versus using all current task samples for training with equal weights. The results for the MNIST and Biased MNIST datasets are shown in Table 4. The results for DP disparity and other datasets, which are similar, are in Sec. B.11. As a result, applying sample weighting to the current task data is necessary to improve fairness while maintaining comparable accuracy.

We also investigate how optimizing for one fairness metric influences other metrics in Table 5 and Sec. B.12. Optimizing FSW for a particular fairness metric partially mitigates disparities in other metrics for EO and DP, since both metrics utilize explicitly defined sensitive attributes, though its effectiveness is generally the highest for the targeted metric. In contrast, FSW does not effectively reduce EER disparity, where the sensitive attribute is defined based on the class label rather than an explicitly defined sensitive attribute.

4.5 Integrating FSW with Fair Post-processing

To answer RQ3, we emphasize the extensibility of FSW by combining it with a state-of-the-art fair post-processing technique for multi-class tasks, ϵ -fair [28]. Since ϵ -fair supports DP, we only report DP results of the Biased MNIST and DRUG datasets in Table 6.

Table 6: Accuracy and fairness (DP disparity) results when combining fair post-processing technique (ϵ -fair) with continual learning methods (iCaRL, WA, OCS, and FSW).

Methods	Biased MNIST		DRUG	
	Acc.	DP Disp.	Acc.	DP Disp.
iCaRL	.802 \pm .008	.015 \pm .001	.444\pm.025	.093 \pm .009
WA	.916 \pm .002	.009 \pm .001	.408 \pm .022	.067 \pm .013
OCS	.824 \pm .007	.035 \pm .003	.393 \pm .017	.053 \pm .012
FSW	.904\pm.004	.008\pm.001	.405 \pm .013	.043 \pm .004
iCaRL – ϵ -fair	<u>.944\pm.008</u>	<u>.006\pm.002</u>	<u>.427\pm.018</u>	<u>.026\pm.004</u>
WA – ϵ -fair	.953\pm.003	<u>.006\pm.002</u>	.404 \pm .021	.044 \pm .020
OCS – ϵ -fair	.952\pm.003	<u>.032\pm.004</u>	.384 \pm .009	.051 \pm .002
FSW – ϵ-fair	.906 \pm .006	.005\pm.001	.405 \pm .013	.021\pm.004

More results and explanations are in Sec. B.13. Comparing original continual learning methods with their integration of ϵ -fair reduces fairness disparity, while accuracy sometimes degrades. This result shows that combining the fair post-processing technique can further improve fairness after model training with continual learning methods. In addition, FSW still shows a better accuracy-fairness tradeoff than existing continual learning methods, even when combined with the fair post-processing technique, compared to existing continual learning methods.

5 Conclusion

We proposed FSW, a fairness-aware sample weighting algorithm for class-incremental learning. Unlike conventional class-incremental learning, we demonstrated how training with all the current task data using equal weights may result in unfair catastrophic forgetting. We theoretically showed that the average gradient vector of the current task data should not oppose the average gradient vector of a sensitive group to avoid unfair forgetting. We then proposed FSW as a solution to adjust the average gradient vector of the current task data, thereby achieving better accuracy-fairness tradeoff results. FSW supports various group fairness measures by converting the optimization problem into a linear program. In our experiments, FSW consistently outperformed baselines in fairness while maintaining comparable accuracy across diverse datasets from various domains. Future work includes generalizing to multiple sensitive attributes, exploring strategies to further reduce computational overhead, and possible strategies of FSW when data drift occurs. Further discussion and analysis of these future directions are provided in Sec. D.

Limitations. Efforts to improve fairness inevitably result in a decrease in accuracy. Despite this inherent trade-off, FSW effectively minimizes the accuracy drop and achieves the best accuracy-fairness tradeoff among all other evaluated approaches (see Sec. 4.2 and B.7 for more details). Additionally, our theoretical analysis relies on a first-order Taylor approximation, which may introduce approximation errors. While higher-order Taylor approximations could theoretically yield more accurate results, they render the optimization problem non-convex and NP-hard. Empirical analysis further demonstrates that the approximation error diminishes rapidly over

training epochs, indicating that our method effectively mitigates approximation inaccuracies introduced by the approximation over time (see Sec. A.3 and B.2 for more details, respectively).

Acknowledgments

This material is based on work that is partially funded by an unrestricted gift from Google. This work was supported by the Institute of Information & Communications Technology Planning & Evaluation (IITP) grant funded by the Korea government (MSIT) (No. RS-2022-II220157, Robust, Fair, Extensible Data-Centric Continual Learning). This work was supported by the Institute of Information & Communications Technology Planning & Evaluation (IITP) grant funded by the Korea government (MSIT) (No. RS-2024-00444862, Non-invasive near-infrared based AI technology for the diagnosis and treatment of brain diseases).

References

- [1] Wickliffe C. Abraham and Anthony Robins. 2005. Memory retention – the synaptic stability versus plasticity dilemma. *Trends in Neurosciences* 28, 2 (2005), 73–78.
- [2] Alekh Agarwal, Alina Beygelzimer, Miroslav Dudík, John Langford, and Hanna M. Wallach. 2018. A Reductions Approach to Fair Classification. In *ICML*, Vol. 80. 60–69.
- [3] Ibrahim M. Alabdulmohsin, Jessica Schrouff, and Sanmi Koyejo. 2022. A Reduction to Binary Approach for Debiasing Multiclass Datasets. In *NeurIPS*.
- [4] Rahaf Aljundi, Min Lin, Baptiste Goujaud, and Yoshua Bengio. 2019. Gradient based sample selection for online continual learning. In *NeurIPS*. 11816–11825.
- [5] Hadis Anahideh, Abolfazl Asudeh, and Saravanan Thirumuruganathan. 2022. Fair active learning. *Expert Systems with Applications* 199 (2022), 116981.
- [6] Julia Angwin, Jeff Larson, Surya Mattu, and Lauren Kirchner. 2016. Machine bias: There’s software used across the country to predict future criminals. And it’s biased against blacks.
- [7] Julia Angwin, Jeff Larson, Surya Mattu, and Lauren Kirchner. 2022. Machine bias. In *Ethics of data and analytics*. 254–264.
- [8] Mohammad Asghari, Amir M. Fathollahi-Fard, S. M. J. Mirzapour Al-e hashem, and Maxim A. Dulebenets. 2022. Transformation and Linearization Techniques in Optimization: A State-of-the-Art Survey. *Mathematics* 10, 2 (2022).
- [9] Jordan T. Ash, Chicheng Zhang, Akshay Krishnamurthy, John Langford, and Alekh Agarwal. 2020. Deep Batch Active Learning by Diverse, Uncertain Gradient Lower Bounds. In *ICLR*.
- [10] Hyojin Bahng, Sanghyuk Chun, Sangdoon Yun, Jaegul Choo, and Seong Joon Oh. 2020. Learning De-biased Representations with Biased Representations. In *ICML*, Vol. 119. 528–539.
- [11] Amir Beck. 2017. *First-order methods in optimization*. SIAM.
- [12] Eden Belouadah, Adrian Popescu, and Ioannis Kanellos. 2021. A comprehensive study of class incremental learning algorithms for visual tasks. *Neural Networks* 135 (2021), 38–54.
- [13] Robert E. Bixby. 2002. Solving Real-World Linear Programs: A Decade and More of Progress. *Oper. Res.* 50, 1 (2002), 3–15.
- [14] Pietro Buzzega, Matteo Boschini, Angelo Porrello, Davide Abati, and Simone Calderara. 2020. Dark Experience for General Continual Learning: a Strong, Simple Baseline. In *NeurIPS*.
- [15] Flávio P. Calmon, Dennis Wei, Bhanukiran Vinzamuri, Karthikeyan Natesan Ramamurthy, and Kush R. Varshney. 2017. Optimized Pre-Processing for Discrimination Prevention. In *NIPS*. 3992–4001.
- [16] Junyi Chai and Xiaoqian Wang. 2022. Fairness with adaptive weights. In *ICML*. PMLR, 2853–2866.
- [17] Arslan Chaudhry, Puneet Kumar Dokania, Thalaiyasingam Ajanthan, and Philip H. S. Torr. 2018. Riemannian Walk for Incremental Learning: Understanding Forgetting and Intransigence. In *ECCV*, Vol. 11215. 556–572.
- [18] Arslan Chaudhry, Albert Gordo, Puneet K. Dokania, Philip H. S. Torr, and David Lopez-Paz. 2021. Using Hindsight to Anchor Past Knowledge in Continual Learning. In *AAAI*. 6993–7001.
- [19] Arslan Chaudhry, Marc’Aurelio Ranzato, Marcus Rohrbach, and Mohamed Elhoseiny. 2019. Efficient Lifelong Learning with A-GEM. In *ICLR*.
- [20] Arslan Chaudhry, Marcus Rohrbach, Mohamed Elhoseiny, Thalaiyasingam Ajanthan, Puneet Kumar Dokania, Philip H. S. Torr, and Marc’Aurelio Ranzato. 2019. Continual Learning with Tiny Episodic Memories. *CoRR* abs/1902.10486 (2019).
- [21] Somnath Basu Roy Chowdhury and Snigdha Chaturvedi. 2023. Sustaining Fairness via Incremental Learning. In *AAAI*. 6797–6805.
- [22] Nikhil Churamani, Ozgur Kara, and Hatice Gunes. 2023. Domain-Incremental Continual Learning for Mitigating Bias in Facial Expression and Action Unit Recognition. *IEEE Trans. Affect. Comput.* 14, 4 (2023), 3191–3206.
- [23] Evgenii Chzhen, Christophe Denis, Mohamed Hebri, Luca Oneto, and Massimiliano Pontil. 2019. Leveraging Labeled and Unlabeled Data for Consistent Fair Binary Classification. In *NeurIPS*. 12739–12750.
- [24] cjadams, Daniel Borkan, inversion, Jeffrey Sorensen, Lucas Dixon, Lucy Vasserman, and nithum. 2019. Jigsaw Unintended Bias in Toxicity Classification. Kaggle.
- [25] Andrew Cotter, Heinrich Jiang, and Karthik Sridharan. 2019. Two-Player Games for Efficient Non-Convex Constrained Optimization. In *ALT*, Vol. 98. 300–332.
- [26] IBM ILOG Cplex. 2009. V12. 1: User’s Manual for CPLEX. *International Business Machines Corporation* 46, 53 (2009), 157.
- [27] Maria De-Arteaga, Alexey Romanov, Hanna M. Wallach, Jennifer T. Chayes, Christian Borgs, Alexandra Chouldechova, Sahin Cem Geyik, Krishnaram Kenthapadi, and Adam Tauman Kalai. 2019. Bias in Bios: A Case Study of Semantic Representation Bias in a High-Stakes Setting. In *FAT*. 120–128.
- [28] Christophe Denis, Romuald Elie, Mohamed Hebri, and François Hu. 2023. Fairness guarantee in multi-class classification. arXiv:2109.13642
- [29] Jacob Devlin, Ming-Wei Chang, Kenton Lee, and Kristina Toutanova. 2019. BERT: Pre-training of Deep Bidirectional Transformers for Language Understanding. In *NAACL-HLT*. 4171–4186.
- [30] Michele Donini, Luca Oneto, Shai Ben-David, John Shawe-Taylor, and Massimiliano Pontil. 2018. Empirical Risk Minimization Under Fairness Constraints. In *NeurIPS*. 2796–2806.
- [31] Sebastian Farquhar and Yarin Gal. 2018. Towards Robust Evaluations of Continual Learning. *CoRR* abs/1805.09733 (2018).
- [32] E. Fehrman, A. K. Muhammad, E. M. Mirkes, V. Egan, and A. N. Gorban. 2017. The Five Factor Model of personality and evaluation of drug consumption risk. arXiv:1506.06297
- [33] Michael Feldman, Sorelle A. Friedler, John Moeller, Carlos Scheidegger, and Suresh Venkatasubramanian. 2015. Certifying and Removing Disparate Impact. In *KDD*. 259–268.
- [34] Robert O. Ferguson and Lauren F. Sargent. 1958. *Linear Programming: Fundamentals and Applications*. McGraw-Hill.
- [35] João Gama, André Žliobaitė, Albert Bifet, Mykola Pechenizkiy, and Abdelhamid Bouchachia. 2014. A survey on concept drift adaptation. *ACM computing surveys (CSUR)* 46, 4 (2014), 1–37.
- [36] Jared Lee Gearhart, Kristin Lynn Adair, Justin David Durfee, Katherine A Jones, Nathaniel Martin, and Richard Joseph Detry. 2013. *Comparison of open-source linear programming solvers*. Technical Report. Sandia National Lab. (SNL-NM), Albuquerque, NM (United States).
- [37] Soumyajit Gupta, Venelin Kovatchev, Maria De-Arteaga, and Matthew Lease. 2024. Fairly accurate: Optimizing accuracy parity in fair target-group detection. *arXiv preprint arXiv:2407.11933* (2024).
- [38] Moritz Hardt, Eric Price, and Nati Srebro. 2016. Equality of Opportunity in Supervised Learning. In *NIPS*. 3315–3323.
- [39] Jiangpeng He. 2024. Gradient reweighting: Towards imbalanced class-incremental learning. In *CVPR*. 16668–16677.
- [40] Qi Huangfu and JA Julian Hall. 2018. Parallelizing the dual revised simplex method. *Mathematical Programming Computation* 10, 1 (2018), 119–142.
- [41] Heinrich Jiang and Ofir Nachum. 2020. Identifying and Correcting Label Bias in Machine Learning. In *AISTATS*, Vol. 108. 702–712.
- [42] Sangwon Jung, Taeon Park, Sanghyuk Chun, and Taesup Moon. 2023. Reweighting based group fairness regularization via classwise robust optimization. *arXiv preprint arXiv:2303.00442* (2023).
- [43] Faisal Kamiran and Toon Calders. 2011. Data preprocessing techniques for classification without discrimination. *Knowl. Inf. Syst.* 33, 1 (2011), 1–33.
- [44] Angelos Katharopoulos and François Fleuret. 2018. Not All Samples Are Created Equal: Deep Learning with Importance Sampling. In *ICML*, Vol. 80. 2530–2539.
- [45] Davinder Kaur, Suleyman Uslu, Kaley J. Rittichier, and Arjan Durresi. 2023. Trustworthy Artificial Intelligence: A Review. *ACM Comput. Surv.* 55, 2 (2023), 39:1–39:38.
- [46] Michael Kearns, Seth Neel, Aaron Roth, and Zhiwei Steven Wu. 2018. Preventing fairness gerrymandering: Auditing and learning for subgroup fairness. In *ICML*. PMLR, 2564–2572.
- [47] KrishnaTeja Killamsetty, Durga Sivasubramanian, Ganesh Ramakrishnan, Abir De, and Rishabh K. Iyer. 2021. GRAD-MATCH: Gradient Matching based Data Subset Selection for Efficient Deep Model Training. In *ICML*, Vol. 139. 5464–5474.
- [48] KrishnaTeja Killamsetty, Durga Sivasubramanian, Ganesh Ramakrishnan, and Rishabh K. Iyer. 2021. GLISTER: Generalization based Data Subset Selection for Efficient and Robust Learning. In *AAAI*. 8110–8118.
- [49] Dongwan Kim and Bohyung Han. 2023. On the Stability-Plasticity Dilemma of Class-Incremental Learning. In *CVPR*. 20196–20204.
- [50] Minsu Kim, Seonghyeon Hwang, and Steven Euijong Whang. 2024. Quilt: Robust Data Segment Selection against Concept Drifts. In *AAAI*. 21249–21257.
- [51] James Kirkpatrick, Razvan Pascanu, Neil C. Rabinowitz, Joel Veness, Guillaume Desjardins, Andrei A. Rusu, Kieran Milan, John Quan, Tiago Ramalho, Agnieszka Grabska-Barwinska, Demis Hassabis, Claudia Clopath, Dharshan Kumaran, and Raia Hadsell. 2016. Overcoming catastrophic forgetting in neural networks.

- CoRR abs/1612.00796 (2016).
- [52] Ron Kohavi. 1996. Scaling Up the Accuracy of Naive-Bayes Classifiers: A Decision-Tree Hybrid. In *KDD*. 202–207.
- [53] Matthias De Lange, Rahaf Aljundi, Marc Masana, Sarah Parisot, Xu Jia, Ales Leonardis, Gregory G. Slabaugh, and Tinne Tuytelaars. 2022. A Continual Learning Survey: Defying Forgetting in Classification Tasks. *IEEE Trans. Pattern Anal. Mach. Intell.* 44, 7 (2022), 3366–3385.
- [54] Yann LeCun, Léon Bottou, Yoshua Bengio, and Patrick Haffner. 1998. Gradient-based learning applied to document recognition. *Proc. IEEE* 86, 11 (1998), 2278–2324.
- [55] Jaehoon Lee, Lechao Xiao, Samuel S. Schoenholz, Yasaman Bahri, Roman Novak, Jascha Sohl-Dickstein, and Jeffrey Pennington. 2019. Wide Neural Networks of Any Depth Evolve as Linear Models Under Gradient Descent. In *NeurIPS*. 8570–8581.
- [56] Haochen Liu, Yiqi Wang, Wenqi Fan, Xiaorui Liu, Yaxin Li, Shaili Jain, Anil K. Jain, and Jiliang Tang. 2021. Trustworthy AI: A Computational Perspective. CoRR abs/2107.06641 (2021).
- [57] Ziwei Liu, Ping Luo, Xiaogang Wang, and Xiaoou Tang. 2015. Deep Learning Face Attributes in the Wild. In *ICCV*. 3730–3738.
- [58] David Lopez-Paz and Marc Aurelio Ranzato. 2017. Gradient Episodic Memory for Continual Learning. In *NIPS*. 6467–6476.
- [59] Songtao Lu, Ioannis C. Tsaknakis, Mingyi Hong, and Yongxin Chen. 2020. Hybrid Block Successive Approximation for One-Sided Non-Convex Min-Max Problems: Algorithms and Applications. *IEEE Trans. Signal Process.* 68 (2020), 3676–3691.
- [60] Zheda Mai, Ruiwen Li, Jihwan Jeong, David Quispe, Hyunwoo Kim, and Scott Sanner. 2022. Online continual learning in image classification: An empirical survey. *Neurocomputing* 469 (2022), 28–51.
- [61] Marc Masana, Xialei Liu, Bartłomiej Twardowski, Mikel Menta, Andrew D. Bagdanov, and Joost van de Weijer. 2023. Class-Incremental Learning: Survey and Performance Evaluation on Image Classification. *IEEE Trans. Pattern Anal. Mach. Intell.* 45, 5 (2023), 5513–5533.
- [62] Bruce A. McCarl and Thomas H. Spreen. 1997. Applied mathematical programming using algebraic systems. *Cambridge, MA* (1997), 524–532.
- [63] Michael McCloskey and Neal J. Cohen. 1989. Catastrophic Interference in Connectionist Networks: The Sequential Learning Problem. *Psychology of Learning and Motivation*, Vol. 24. 109–165.
- [64] Ninareh Mehrabi, Fred Morstatter, Nripsuta Saxena, Kristina Lerman, and Aram Galstyan. 2022. A Survey on Bias and Fairness in Machine Learning. *ACM Comput. Surv.* 54, 6 (2022), 115:1–115:35.
- [65] Martial Mermillod, Aurélie Bugaiska, and Patrick BONIN. 2013. The stability-plasticity dilemma: investigating the continuum from catastrophic forgetting to age-limited learning effects. *Frontiers in Psychology* 4 (2013).
- [66] Seyed-Iman Mirzadeh, Mehrdad Farajtabar, Razvan Pascanu, and Hassan Ghasemzadeh. 2020. Understanding the Role of Training Regimes in Continual Learning. In *NeurIPS*.
- [67] Baharan Mirzasoileiman, Jeff A. Bilmes, and Jure Leskovec. 2020. Coresets for Data-efficient Training of Machine Learning Models. In *ICML*, Vol. 119. 6950–6960.
- [68] Jinlong Pang, Jialu Wang, Zhaowei Zhu, Yuanshun Yao, Chen Qian, and Yang Liu. 2024. Fairness Without Harm: An Influence-Guided Active Sampling Approach. In *NeurIPS*.
- [69] Panos M. Pardalos and Stephen A. Vavasis. 1991. Quadratic programming with one negative eigenvalue is NP-hard. *Journal of Global optimization* 1, 1 (1991), 15–22.
- [70] German Ignacio Parisi, Ronald Kemker, Jose L. Part, Christopher Kanan, and Stefan Wermter. 2019. Continual lifelong learning with neural networks: A review. *Neural Networks* 113 (2019), 54–71.
- [71] Geoff Pleiss, Manish Raghavan, Felix Wu, Jon M. Kleinberg, and Kilian Q. Weinberger. 2017. On Fairness and Calibration. In *NIPS*. 5680–5689.
- [72] Preston Putzel and Scott Lee. 2022. Blackbox post-processing for multiclass fairness. *arXiv preprint arXiv:2201.04461* (2022).
- [73] Sylvestre-Alvise Rebuffi, Alexander Kolesnikov, Georg Sperl, and Christoph H. Lampert. 2017. iCaRL: Incremental Classifier and Representation Learning. In *CVPR*. 5533–5542.
- [74] Yuji Roh, Kangwook Lee, Steven Whang, and Changho Suh. 2020. FR-Train: A Mutual Information-Based Approach to Fair and Robust Training. In *ICML*, Vol. 119. 8147–8157.
- [75] Yuji Roh, Kangwook Lee, Steven Euijong Whang, and Changho Suh. 2021. Fair-Batch: Batch Selection for Model Fairness. In *ICLR*.
- [76] Yuji Roh, Weli Nie, De-An Huang, Steven Euijong Whang, Arash Vahdat, and Anima Anandkumar. 2023. Dr-Fairness: Dynamic Data Ratio Adjustment for Fair Training on Real and Generated Data. *Transactions on Machine Learning Research* (2023).
- [77] David Sculley. 2010. Web-scale k-means clustering. In *Proceedings of the 19th international conference on World wide web*. 1177–1178.
- [78] Aili Shen, Xudong Han, Trevor Cohn, Timothy Baldwin, and Lea Frermann. 2022. Optimising Equal Opportunity Fairness in Model Training. In *NAACL*. 4073–4084.
- [79] Srikrishna Sridhar, Stephen Wright, Christopher Re, Ji Liu, Victor Bittorf, and Ce Zhang. 2013. An approximate, efficient LP solver for LP rounding. *Advances in Neural Information Processing Systems* 26 (2013).
- [80] Ki Hyun Tae, Hantian Zhang, Jaeyoung Park, Kexin Rong, and Steven Euijong Whang. 2024. Falcon: Fair Active Learning Using Multi-Armed Bandits. *Proceedings of the VLDB Endowment* 17, 5 (2024), 952–965.
- [81] Thanh-Dat Truong, Hoang-Quan Nguyen, Bhiksha Raj, and Khoa Luu. 2023. Fairness Continual Learning Approach to Semantic Scene Understanding in Open-World Environments. In *NeurIPS*.
- [82] Gido M. van de Ven and Andreas S. Tolias. 2019. Three scenarios for continual learning. CoRR abs/1904.07734 (2019).
- [83] Suresh Venkatasubramanian. 2019. Algorithmic Fairness: Measures, Methods and Representations. In *PODS*. 481.
- [84] Fu-Yun Wang, Da-Wei Zhou, Han-Jia Ye, and De-Chuan Zhan. 2022. FOSTER: Feature Boosting and Compression for Class-Incremental Learning. In *ECCV*, Vol. 13685. 398–414.
- [85] Zifeng Wang, Zizhao Zhang, Chen-Yu Lee, Han Zhang, Ruoxi Sun, Xiaoqi Ren, Guolong Su, Vincent Perot, Jennifer Dy, and Tomas Pfister. 2022. Learning to prompt for continual learning. In *Proceedings of the IEEE/CVF conference on computer vision and pattern recognition*. 139–149.
- [86] Yue Wu, Yinpeng Chen, Lijuan Wang, Yuancheng Ye, Zicheng Liu, Yandong Guo, and Yun Fu. 2019. Large Scale Incremental Learning. In *CVPR*. 374–382.
- [87] Han Xiao, Kashif Rasul, and Roland Vollgraf. 2017. Fashion-MNIST: a Novel Image Dataset for Benchmarking Machine Learning Algorithms. CoRR abs/1708.07747 (2017).
- [88] Shixiong Xu, Gaofeng Meng, Xing Nie, Bolin Ni, Bin Fan, and Shiming Xiang. 2024. Defying Imbalanced Forgetting in Class Incremental Learning. In *AAAI*, Vol. 38. 16211–16219.
- [89] Tian Xu, Jennifer White, Sinan Kalkan, and Hatice Gunes. 2020. Investigating Bias and Fairness in Facial Expression Recognition. In *ECCV*, Vol. 12540. 506–523.
- [90] Shipeng Yan, Jiangwei Xie, and Xuming He. 2021. DER: Dynamically expandable representation for class incremental learning. In *Proceedings of the IEEE/CVF conference on computer vision and pattern recognition*. 3014–3023.
- [91] Shipeng Yan, Jiangwei Xie, and Xuming He. 2021. DER: Dynamically Expandable Representation for Class Incremental Learning. In *CVPR*. 3014–3023.
- [92] Jaehong Yoon, Divyam Madaan, Eunho Yang, and Sung Ju Hwang. 2022. Online Coreset Selection for Rehearsal-based Continual Learning. In *ICLR*.
- [93] Brian Hu Zhang, Blake Lemoine, and Margaret Mitchell. 2018. Mitigating Unwanted Biases with Adversarial Learning. In *AIES*. 335–340.
- [94] Hantian Zhang, Ki Hyun Tae, Jaeyoung Park, Xu Chu, and Steven Euijong Whang. 2023. iflipper: Label flipping for individual fairness. *Proceedings of the ACM on Management of Data* 1, 1 (2023), 1–26.
- [95] Bowen Zhao, Xi Xiao, Guojun Gan, Bin Zhang, and Shu-Tao Xia. 2020. Maintaining Discrimination and Fairness in Class Incremental Learning. In *CVPR*. 13205–13214.
- [96] Da-Wei Zhou, Qi-Wei Wang, Zhi-Hong Qi, Han-Jia Ye, De-Chuan Zhan, and Ziwei Liu. 2023. Deep Class-Incremental Learning: A Survey. CoRR abs/2302.03648 (2023).
- [97] Da-Wei Zhou, Qi-Wei Wang, Han-Jia Ye, and De-Chuan Zhan. 2023. A Model or 603 Exemplars: Towards Memory-Efficient Class-Incremental Learning. In *ICLR*.
- [98] Da-Wei Zhou, Qi-Wei Wang, Zhi-Hong Qi, Han-Jia Ye, De-Chuan Zhan, and Ziwei Liu. 2024. Class-incremental learning: A survey. *IEEE Transactions on Pattern Analysis and Machine Intelligence* (2024).
- [99] Huiping Zhuang, Yue Yan, Run He, and Ziqian Zeng. 2024. Class incremental learning with analytic learning for hyperspectral image classification. *Journal of the Franklin Institute* 361, 18 (2024), 107285.

A Technical Appendices

A.1 Notations used in the paper

Continuing from Sec. 3, Table 7 summarizes the notations used in our paper to enhance readability.

Table 7: Summary of notations used throughout the paper.

Symbol	Description
X	Feature of a data point.
y or y	True label of a data point.
\hat{y} or \hat{y}	Predicted label of a data point.
z or z	Sensitive attribute of a data point.
d	Data point including X and y .
\mathbb{Y}	Set of all classes.
\mathbb{Y}_c	Set of classes in current task.
\mathbb{Z}	Set of sensitive attributes.
L	Total number of tasks.
l	Index of current task.
T_l	Dataset for current task l (including d).
w_l	Training weight of current task l .
M_l	Buffer data for current task l .
N	Number of classes in each task.
M	Size of buffer.
m	Number of samples of buffer data per task.
G	Sensitive group.
G_y	Sensitive group with label y .
$G_{y,z}$	Sensitive group with label y and sensitive attribute z .
$G_{\mathbb{Y}}$	Average of all G_y .
θ	Model parameters.
f_{θ}^{l-1}	Model for previous task $l-1$.
f_{θ}	Current Model.
ℓ or \mathcal{L}	Loss function.
$\tilde{\ell}$	Approximated loss function.
$\ell(f_{\theta}, G)$	Average loss for the samples in the group G .
$\nabla \ell(f_{\theta}, G)$	Average gradient vector for the samples in the group G .
$\nabla \ell(f_{\theta}, d)$	Average gradient vector for a sample d .
η	Model learning rate.
α	Hyperparameter that determines the model update rate during optimization.
λ	Hyperparameter that balances accuracy and fairness.
τ	Hyperparameter that balances previous and current task samples.

A.2 Theoretical Analysis of Unfairness in Class-Incremental Learning

Continuing from Sec. 3.1, we prove the lemma on the updated loss of a group of data after learning the current task data.

LEMMA A.1 (RESTATED FROM LEMMA 3.1). *Denote G as a sensitive group containing features X and true labels y . Also, denote f_{θ}^{l-1} as a previous model and f_{θ} as the updated model after training on the current task T_l . Let ℓ be any differentiable loss function (e.g., cross-entropy loss), and η be a learning rate. Then, the loss of the sensitive group of data after training with a current task sample $d_i \in T_l$ is approximated as follows:*

$$\tilde{\ell}(f_{\theta}, G) = \ell(f_{\theta}^{l-1}, G) - \eta \nabla_{\theta} \ell(f_{\theta}^{l-1}, G)^{\top} \nabla_{\theta} \ell(f_{\theta}^{l-1}, d_i),$$

where $\tilde{\ell}(f_{\theta}, G)$ is the approximated average loss between model predictions $f_{\theta}(X)$ and true labels y , whereas $\ell(f_{\theta}^{l-1}, G)$ is the exact average loss, $\nabla_{\theta} \ell(f_{\theta}^{l-1}, G)$ is the average gradient vector for the samples in the group G , and $\nabla_{\theta} \ell(f_{\theta}^{l-1}, d_i)$ is the gradient vector for a sample d_i , each with respect to the previous model f_{θ}^{l-1} .

PROOF. Assume that the loss can be well approximated by its first-order Taylor expansion around θ^{l-1} . We update the model using gradient descent with the current task sample $d_i \in T_l$ and learning rate η as follows:

$$\theta = \theta^{l-1} - \eta \nabla_{\theta} \ell(f_{\theta}^{l-1}, d_i).$$

Using the Taylor series approximation,

$$\begin{aligned} \tilde{\ell}(f_{\theta}, G) &= \ell(f_{\theta}^{l-1}, G) + \nabla_{\theta} \ell(f_{\theta}^{l-1}, G)^{\top} (\theta - \theta^{l-1}) \\ &= \ell(f_{\theta}^{l-1}, G) + \nabla_{\theta} \ell(f_{\theta}^{l-1}, G)^{\top} (-\eta \nabla_{\theta} \ell(f_{\theta}^{l-1}, d_i)) \\ &= \ell(f_{\theta}^{l-1}, G) - \eta \nabla_{\theta} \ell(f_{\theta}^{l-1}, G)^{\top} \nabla_{\theta} \ell(f_{\theta}^{l-1}, d_i). \end{aligned}$$

If we update the model using all the current task data T_l , the equation is formulated as $\tilde{\ell}(f_{\theta}, G) = \ell(f_{\theta}^{l-1}, G) - \eta \nabla_{\theta} \ell(f_{\theta}^{l-1}, G)^{\top} \nabla_{\theta} \ell(f_{\theta}^{l-1}, T_l)$. Therefore, if the average gradient vectors of the sensitive group and the current task data have opposite directions, i.e., $\nabla_{\theta} \ell(f_{\theta}^{l-1}, G)^{\top} \nabla_{\theta} \ell(f_{\theta}^{l-1}, T_l) < 0$, learning the current task data increases the loss of the sensitive group data and finally leads to catastrophic forgetting. \square

We next derive a sufficient condition for unfair forgetting.

THEOREM A.2 (RESTATED FROM THEOREM 3.3). *Let ℓ be the cross-entropy loss and G_1 and G_2 the overperforming and underperforming sensitive groups of data, respectively. Also let d_i be a training sample that satisfy the following conditions: $\ell(f_{\theta}^{l-1}, G_1) < \ell(f_{\theta}^{l-1}, G_2)$ while $\nabla_{\theta} \ell(f_{\theta}^{l-1}, G_1)^{\top} \nabla_{\theta} \ell(f_{\theta}^{l-1}, d_i) > 0$ and $\nabla_{\theta} \ell(f_{\theta}^{l-1}, G_2)^{\top} \nabla_{\theta} \ell(f_{\theta}^{l-1}, d_i) < 0$. Then $|\tilde{\ell}(f_{\theta}, G_1) - \tilde{\ell}(f_{\theta}, G_2)| > |\ell(f_{\theta}^{l-1}, G_1) - \ell(f_{\theta}^{l-1}, G_2)|$.*

PROOF. Using the derived equation in the lemma A.1 $\tilde{\ell}(f_{\theta}, G) = \ell(f_{\theta}^{l-1}, G) - \eta \nabla_{\theta} \ell(f_{\theta}^{l-1}, G)^{\top} \nabla_{\theta} \ell(f_{\theta}^{l-1}, d_i)$, we compute the disparity of losses between the two groups G_1 and G_2 after the model update as follows:

$$\begin{aligned} &|\tilde{\ell}(f_{\theta}, G_1) - \tilde{\ell}(f_{\theta}, G_2)| \\ &= |(\ell(f_{\theta}^{l-1}, G_1) - \eta \nabla_{\theta} \ell(f_{\theta}^{l-1}, G_1)^{\top} \nabla_{\theta} \ell(f_{\theta}^{l-1}, d_i)) \\ &\quad - (\ell(f_{\theta}^{l-1}, G_2) - \eta \nabla_{\theta} \ell(f_{\theta}^{l-1}, G_2)^{\top} \nabla_{\theta} \ell(f_{\theta}^{l-1}, d_i))| \\ &= |(\ell(f_{\theta}^{l-1}, G_1) - \ell(f_{\theta}^{l-1}, G_2)) \\ &\quad - \eta (\nabla_{\theta} \ell(f_{\theta}^{l-1}, G_1)^{\top} \nabla_{\theta} \ell(f_{\theta}^{l-1}, d_i) - \nabla_{\theta} \ell(f_{\theta}^{l-1}, G_2)^{\top} \nabla_{\theta} \ell(f_{\theta}^{l-1}, d_i))|. \end{aligned}$$

Since $\ell(f_{\theta}^{l-1}, G_1) < \ell(f_{\theta}^{l-1}, G_2)$, it leads to $\ell(f_{\theta}^{l-1}, G_1) - \ell(f_{\theta}^{l-1}, G_2) < 0$. Next, the two assumptions of $\nabla_{\theta} \ell(f_{\theta}^{l-1}, G_1)^{\top} \nabla_{\theta} \ell(f_{\theta}^{l-1}, d_i) > 0$ and $\nabla_{\theta} \ell(f_{\theta}^{l-1}, G_2)^{\top} \nabla_{\theta} \ell(f_{\theta}^{l-1}, d_i) < 0$ make $-\eta (\nabla_{\theta} \ell(f_{\theta}^{l-1}, G_1)^{\top} \nabla_{\theta} \ell(f_{\theta}^{l-1}, d_i) - \nabla_{\theta} \ell(f_{\theta}^{l-1}, G_2)^{\top} \nabla_{\theta} \ell(f_{\theta}^{l-1}, d_i)) < 0$. Since the two terms in the absolute value equation are both negative,

$$\begin{aligned} &|\tilde{\ell}(f_{\theta}, G_1) - \tilde{\ell}(f_{\theta}, G_2)| \\ &= |\ell(f_{\theta}^{l-1}, G_1) - \ell(f_{\theta}^{l-1}, G_2)| \\ &\quad + |-\eta (\nabla_{\theta} \ell(f_{\theta}^{l-1}, G_1)^{\top} \nabla_{\theta} \ell(f_{\theta}^{l-1}, d_i) - \nabla_{\theta} \ell(f_{\theta}^{l-1}, G_2)^{\top} \nabla_{\theta} \ell(f_{\theta}^{l-1}, d_i))| \\ &> |\ell(f_{\theta}^{l-1}, G_1) - \ell(f_{\theta}^{l-1}, G_2)|. \end{aligned}$$

We finally have $|\tilde{\ell}(f_\theta, G_1) - \tilde{\ell}(f_\theta, G_2)| > |\ell(f_\theta^{l-1}, G_1) - \ell(f_\theta^{l-1}, G_2)|$, which implies that fairness deteriorates after training on the current task data. \square

A.3 Higher-order approximation for Taylor series

Continuing from Sec. 3.1, we can extend the approximated loss to a higher-order Taylor approximation to improve theoretical accuracy, but it makes the optimization non-convex and NP-hard.

THEOREM A.3. *Employing a second-order Taylor approximation on Lemma 3.1 makes the optimization problem non-convex and NP-hard.*

PROOF. Using a second-order Taylor expansion around the current model parameters θ , the approximated loss becomes:

$$\tilde{\ell}(G) = \ell(G) - \nabla_\theta \ell(G)^\top \mathbf{x} + \frac{1}{2} \mathbf{x}^\top H_\theta(G) \mathbf{x},$$

where $H_\theta(G)$ is the Hessian (assumed to be PSD; we also prove a case when it is not, and we define $\mathbf{x} := \frac{\eta}{|\mathcal{T}|} \sum_{d_i \in \mathcal{T}} \mathbf{w}^i \nabla_\theta \ell(d_i)$). This function is convex in \mathbf{x} and thus convex in \mathbf{w} . To encourage fairness, we penalize the difference between the two group losses:

$$\mathcal{L}_{\text{fair}}(\mathbf{w}) := |\tilde{\ell}(G_1) - \tilde{\ell}(G_2)| = \left| c + b^\top \mathbf{x} + \frac{1}{2} \mathbf{x}^\top Q \mathbf{x} \right|,$$

where c and b are appropriate constants and $Q = H_\theta(G_1) - H_\theta(G_2)$. Introducing a slack variable t , we rewrite the fairness loss constraint as:

$$-t \leq c + b^\top \mathbf{x} + \frac{1}{2} \mathbf{x}^\top Q \mathbf{x} \leq t.$$

This yields a Quadratically Constrained Quadratic Program (QCQP) in \mathbf{w} . The constraint involves a quadratic form with matrix $Q = H_\theta(G_1) - H_\theta(G_2)$. In general, Q is indefinite unless $H_\theta(G_1) = H_\theta(G_2)$. Hence, at least one constraint is non-convex.

It is known that a QCQP, even with a single non-PSD constraint matrix, is non-convex and NP-hard. [69] Although $\tilde{\ell}(G)$ is convex in \mathbf{w} , the fairness term introduces non-convexity. Thus, the overall optimization problem is non-convex and NP-hard.

Furthermore, if $H_\theta(G)$ is not PSD, then $\tilde{\ell}(G)$ itself becomes non-convex in \mathbf{w} , which also leads to an NP-hard optimization problem. \square

A.4 From Cross-Entropy Loss to Group Fairness Metrics

Continuing from Sec. 3.1, we explain how to approximate the group fairness metrics using cross-entropy loss disparity. Existing works [75, 76, 78] empirically demonstrated that using the cross-entropy loss disparity provides reasonable proxies for common group fairness metrics such as equalized odds (EO) and demographic parity (DP) disparity. In addition, we theoretically describe how minimizing the cost function for EO using the cross-entropy loss disparity (i.e., $\mathcal{L}_{EO} = \frac{1}{|\mathcal{Y}||\mathcal{Z}|} \sum_{y \in \mathcal{Y}, z \in \mathcal{Z}} |\ell(f_\theta, G_{y,z}) - \ell(f_\theta, G_y)|$ where ℓ is a cross-entropy loss) leads to ensuring EO disparity. [78] theoretically and empirically showed that using cross-entropy loss instead of the 0-1 loss (i.e., $\mathbb{1}(y \neq \hat{y})$ where $\mathbb{1}(\cdot)$ is an indicator function, which is equivalent to the probability of correct prediction) can still capture EO disparity in binary classification. We now

prove how applying the cross-entropy loss disparity for EO can be extended to multi-class classification as follows:

Let \mathcal{Y} denote the set of all class labels. For each sample i , let $y_i \in \mathcal{Y}$ be its true label, $\hat{y}_i \in \mathcal{Y}$ its predicted label, and z_i its sensitive attribute. Define $m_{y,z} := |\{i : y_i = y, z_i = z\}|$ as the size of a sensitive group. Also, let $(y_i^1, y_i^2, \dots, y_i^{|\mathcal{Y}|})^\top$ and $(\hat{y}_i^1, \hat{y}_i^2, \dots, \hat{y}_i^{|\mathcal{Y}|})^\top$ denote the one-hot encoded vector of the true label y_i and the predicted probability distribution over all classes for sample i , respectively, where $y_i^j \in \{0, 1\}$ and $\hat{y}_i^j \in [0, 1]$ for $j \in [1, 2, \dots, |\mathcal{Y}|]$. Then, the cross-entropy loss for a sensitive group $G_{y,z}$ can be transformed as follows:

$$\begin{aligned} \ell(f_\theta, G_{y,z}) &= -\frac{1}{m_{y,z}} \sum_{i=1}^{m_{y,z}} \left(\sum_{j=1}^{|\mathcal{Y}|} y_i^j \cdot \log(\hat{y}_i^j) \right) \\ &= -\frac{1}{m_{y,z}} \sum_{i=1}^{m_{y,z}} \log(\hat{y}_i^y). \end{aligned}$$

Since \hat{y}_i^y is equivalent to $p(\hat{y}_i = y)$ and we are measuring a loss for the sensitive group ($y = y, z = z$), $\ell(f_\theta, G_{y,z}) = -\frac{1}{m_{y,z}} \sum_i \log(p(\hat{y}_i))$ is an unbiased estimator of $-\log p(\hat{y}|y = y, z = z)$. Likewise, $\ell(f_\theta, G_y)$ is an unbiased estimator of $-\log p(\hat{y}|y = y)$, and our cost function becomes equivalent to $\left| \log \frac{p(\hat{y}|y=y)}{p(\hat{y}|y=y, z=z)} \right|$. Since $\frac{p(\hat{y}|y=y)}{p(\hat{y}|y=y, z=z)} = 1$ for all y, z implies that prediction outcomes are independent of the sensitive attribute given the true label, we conclude that minimizing the cost function for EO can satisfy equalized odds.

We next perform experiments to evaluate how well the cost function for EO approximates EO disparity (i.e., $\frac{1}{|\mathcal{Y}||\mathcal{Z}|} \sum_{y \in \mathcal{Y}, z \in \mathcal{Z}} |\Pr(\hat{y} = y|y = y, z = z) - \Pr(\hat{y} = y|y = y)|$) on the Biased MNIST dataset as shown in Fig. 4. Although the scales of the two metrics are different, the simultaneous movements of these two trends suggest that our cost function is effective in satisfying equalized odds.

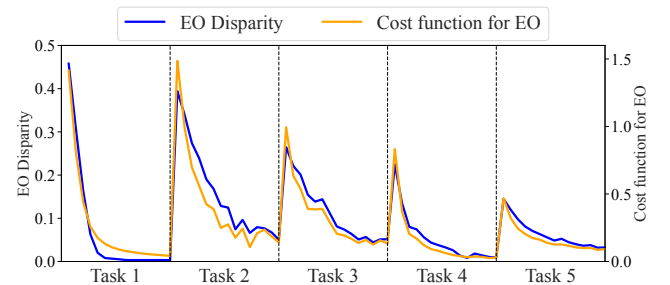


Figure 4: Comparison of EO disparity and cost function for EO during training on the Biased MNIST dataset. We train a model for 15 epochs per task.

We can also extend our theoretical claim to the cost function for EER and DP. In case of EER, $\ell(f_\theta, G_y)$ and $\ell(f_\theta, G_{\bar{y}})$ are unbiased estimators of $-\log p(\hat{y}|y = y)$ and $-\log p(\hat{y})$, respectively. Similarly, for DP, $\ell'(f_\theta, G_{y,z})$ and $\ell'(f_\theta, G_y)$ are unbiased estimators of $-\log p(\hat{y}|z = z)$ and $-\log p(\hat{y})$, respectively.

A.5 Derivation of a Sufficient Condition for Demographic Parity in the Multi-Class Setting

Continuing from Sec. 3.2, we derive a sufficient condition for satisfying demographic parity in the multi-class setting.

PROPOSITION A.4. *In the multi-class setting, $\frac{m_{y,z_1}}{m_{*,z_1}} \ell(f_\theta, G_{y,z_1}) = \frac{m_{y,z_2}}{m_{*,z_2}} \ell(f_\theta, G_{y,z_2})$ where $m_{y,z} := |\{i : y_i = y, z_i = z\}|$ and $m_{*,z} := |\{i : z_i = z\}|$ for $y \in \mathbb{Y}$ and $z_1, z_2 \in \mathbb{Z}$ can serve as a sufficient condition for demographic parity.*

PROOF. In the multi-class setting, we can extend the definition of demographic parity as $\Pr(\hat{y} = y|z = z_1) = \Pr(\hat{y} = y|z = z_2)$ for $y \in \mathbb{Y}$ and $z_1, z_2 \in \mathbb{Z}$. The term $\Pr(\hat{y} = y|z = z)$ can be decomposed as follows: $\Pr(\hat{y} = y|z = z) = \Pr(\hat{y} = y, y = y|z = z) + \sum_{y_n \neq y} \Pr(\hat{y} = y, y = y_n|z = z)$. Without loss of generality, we set $z_1 = 0$ and $z_2 = 1$. Then the definition of demographic parity in the multi-class setting now becomes

$$\begin{aligned} & \Pr(\hat{y} = y, y = y|z = 0) + \sum_{y_n \neq y} \Pr(\hat{y} = y, y = y_n|z = 0) \\ &= \Pr(\hat{y} = y, y = y|z = 1) + \sum_{y_n \neq y} \Pr(\hat{y} = y, y = y_n|z = 1). \end{aligned}$$

The term $\Pr(\hat{y} = y, y = y|z = 0)$ can be represented with the 0-1 loss as follows:

$$\begin{aligned} \Pr(\hat{y} = y, y = y|z = 0) &= \frac{\Pr(\hat{y} = y, y = y, z = 0)}{\Pr(z = 0)} \\ &= \frac{\Pr(\hat{y} = y|y = y, z = 0) \Pr(y = y, z = 0)}{\Pr(z = 0)} \\ &= \frac{1}{m_{*,0}} \sum_{i:y_i=y,z_i=0} (1 - \mathbb{1}(y_i \neq \hat{y}_i)), \end{aligned}$$

where $\mathbb{1}(\cdot)$ is an indicator function. Similarly, $\Pr(\hat{y} = y, y = y_n|z = 0)$ for $y_n \neq y$ can be transformed as follows:

$$\begin{aligned} \Pr(\hat{y} = y, y = y_n|z = 0) &= \frac{\Pr(\hat{y} = y, y = y_n, z = 0)}{\Pr(z = 0)} \\ &= \frac{\Pr(\hat{y} = y|y = y_n, z = 0) \Pr(y = y_n, z = 0)}{\Pr(z = 0)} \\ &= \frac{1}{m_{*,0}} \sum_{j:y_j=y_n,z_j=0} \mathbb{1}(y_j \neq \hat{y}_j). \end{aligned}$$

By applying the same technique to $\Pr(\hat{y} = y, y = y|z = 1)$ and $\Pr(\hat{y} = y, y = y_n|z = 1)$, we have the 0-1 loss-based definition of demographic parity:

$$\begin{aligned} & \frac{1}{m_{*,0}} \sum_{i:y_i=y,z_i=0} (1 - \mathbb{1}(y_i \neq \hat{y}_i)) + \sum_{i:y_i \neq y} \frac{1}{m_{*,0}} \sum_{j:y_j=y_i,z_j=0} \mathbb{1}(y_j \neq \hat{y}_j) \\ &= \frac{1}{m_{*,1}} \sum_{i:y_i=y,z_i=1} (1 - \mathbb{1}(y_i \neq \hat{y}_i)) + \sum_{i:y_i \neq y} \frac{1}{m_{*,1}} \sum_{j:y_j=y_i,z_j=1} \mathbb{1}(y_j \neq \hat{y}_j). \end{aligned}$$

Since the 0-1 loss is not differentiable, it is not suitable to approximate the loss using gradients as in Eq. 1. We thus approximate the 0-1 loss to a standard loss function ℓ (e.g., cross-entropy loss),

$$\begin{aligned} & \frac{1}{m_{*,0}} \sum_{i:y_i=y,z_i=0} -\ell(f_\theta, d_i) + \sum_{i:y_i \neq y} \frac{1}{m_{*,0}} \sum_{j:y_j=y_i,z_j=0} \ell(f_\theta, d_j) \\ &= \frac{1}{m_{*,1}} \sum_{i:y_i=y,z_i=1} -\ell(f_\theta, d_i) + \sum_{i:y_i \neq y} \frac{1}{m_{*,1}} \sum_{j:y_j=y_i,z_j=1} \ell(f_\theta, d_j), \end{aligned}$$

where $\ell(f_\theta, d_j)$ is the loss between the model prediction $f_\theta(d_j)$ and the true label y_j . By replacing $\sum_{i:y_i=y_i,z_i=z} \ell(f_\theta, d_i)$ with $m_{y,z} \ell(f_\theta, G_{y,z})$,

$$\begin{aligned} & \frac{m_{y,0}}{m_{*,0}} (-\ell(f_\theta, G_{y,0})) + \sum_{i:y_i \neq y} \frac{m_{y_i,0}}{m_{*,0}} \ell(f_\theta, G_{y_i,0}) \\ &= \frac{m_{y,1}}{m_{*,1}} (-\ell(f_\theta, G_{y,1})) + \sum_{i:y_i \neq y} \frac{m_{y_i,1}}{m_{*,1}} \ell(f_\theta, G_{y_i,1}). \end{aligned}$$

To satisfy the constraint for all $y \in \mathbb{Y}$, the corresponding terms on the left-hand side and the right-hand side of the equation should be equal, i.e., $\frac{m_{y,0}}{m_{*,0}} \ell(f_\theta, G_{y,0}) = \frac{m_{y,1}}{m_{*,1}} \ell(f_\theta, G_{y,1})$. In general, we derive a sufficient condition for demographic parity as $\frac{m_{y,z_1}}{m_{*,z_1}} \ell(f_\theta, G_{y,z_1}) = \frac{m_{y,z_2}}{m_{*,z_2}} \ell(f_\theta, G_{y,z_2})$. Note that the number of samples in sensitive groups (e.g., $m_{*,z}$ and $m_{y,z}$) is derived from the definition of demographic parity, which is independent of sample weights. \square

A.6 LP Formulation of Fairness-aware Optimization Problems

Continuing from Sec. 3.2, we prove Theorem 3.4, which implies that fairness-aware optimization problems can be transformed into linear programming problems. This transformation is made possible by using Lemma A.5, which suggests that minimizing the sum of absolute values with linear terms can be transformed into a linear programming form.

LEMMA A.5. *The following optimization problem can be reformulated into a linear programming form. Note that in the following equation, y and z refer to arbitrary variables, not to the label or sensitive attribute, respectively.*

$$\begin{aligned} & \min_{\mathbf{x}} \sum_{i=1}^n |y_i| + z_i \\ \text{s.t. } & y_i = a_i - \mathbf{b}_i^\top \mathbf{x}, \quad z_i = c_i - \mathbf{d}_i^\top \mathbf{x} \\ & a_i, c_i, y_i, z_i \in \mathbb{R}, \quad \mathbf{b}_i, \mathbf{d}_i \in \mathbb{R}^{m \times 1}, \quad \forall i \in \{1, \dots, n\}, \quad \mathbf{x} \in [0, 1]^{m \times 1}. \end{aligned}$$

PROOF. The transformation for minimizing the sum of absolute values was introduced in [8, 34, 62]. Note that considering the additional affine term does not affect the flow of the proof. We first substitute y_i for $y_i^+ - y_i^-$ where both y_i^+ and y_i^- are nonnegative. Then, the optimization problem becomes

$$\begin{aligned} & \min_{\mathbf{x}} \sum_{i=1}^n |y_i^+ - y_i^-| + z_i \\ \text{s.t. } & y_i^+ - y_i^- = a_i - \mathbf{b}_i^\top \mathbf{x}, \quad z_i = c_i - \mathbf{d}_i^\top \mathbf{x}, \\ & y_i^+ - y_i^- = y_i, \quad y_i^+, y_i^- \in \mathbb{R}^+, \\ & a_i, c_i, y_i, z_i \in \mathbb{R}, \quad \mathbf{b}_i, \mathbf{d}_i \in \mathbb{R}^{m \times 1}, \quad \forall i \in \{1, \dots, n\}, \quad \mathbf{x} \in [0, 1]^{m \times 1}. \end{aligned}$$

This problem is still nonlinear. However, the absolute value terms can be simplified when either y_i^+ or y_i^- equals to zero (i.e., $y_i^+ y_i^- = 0$), as the consequent absolute value reduces to zero plus the other

term. Then, the absolute value term can be written as the sum of two variables,

$$|y_i^+ - y_i^-| = |y_i^+| + |y_i^-| = y_i^+ + y_i^- \quad \text{if } y_i^+ y_i^- = 0.$$

By using the assumption, the formulation becomes

$$\begin{aligned} & \min_{\mathbf{x}} \sum_{i=1}^n y_i^+ + y_i^- + z_i \\ \text{s.t. } & y_i^+ - y_i^- = a_i - \mathbf{b}_i^\top \mathbf{x}, \quad z_i = c_i - \mathbf{d}_i^\top \mathbf{x}, \\ & y_i^+ - y_i^- = y_i, \quad y_i^+ y_i^- = 0, \quad y_i^+, y_i^- \in \mathbb{R}^+, \\ & a_i, c_i, y_i, z_i \in \mathbb{R}, \quad \mathbf{b}_i, \mathbf{d}_i \in \mathbb{R}^{m \times 1}, \quad \forall i \in \{1, \dots, n\}, \quad \mathbf{x} \in [0, 1]^{m \times 1}, \end{aligned}$$

with the underlined condition added. However, this condition can be dropped. Assume there exist y_i^+ and y_i^- , which do not satisfy $y_i^+ y_i^- = 0$. When $y_i^+ \geq y_i^- > 0$, there exists a better solution $(y_i^+ - y_i^-, 0)$ instead of (y_i^+, y_i^-) , which satisfies all the conditions, but has a smaller objective function value $y_i^+ - y_i^- + 0 + z_i < y_i^+ + y_i^- + z_i$. For the case of $y_i^- > y_i^+ > 0$, a solution $(0, y_i^- - y_i^+)$ works better for similar reasons. Thus, the minimization automatically leads to $y_i^+ y_i^- = 0$, and the underlined nonlinear constraint becomes unnecessary. Consequently, the final formulation becomes LP:

$$\begin{aligned} & \min_{\mathbf{x}} \sum_{i=1}^n y_i^+ + y_i^- + z_i \\ \text{s.t. } & y_i^+ - y_i^- = a_i - \mathbf{b}_i^\top \mathbf{x}, \quad z_i = c_i - \mathbf{d}_i^\top \mathbf{x}, \\ & y_i^+ - y_i^- = y_i y_i^+, \quad y_i^- \in \mathbb{R}^+, \\ & a_i, c_i, y_i, z_i \in \mathbb{R}, \quad \mathbf{b}_i, \mathbf{d}_i \in \mathbb{R}^{m \times 1}, \quad \forall i \in \{1, \dots, n\}, \quad \mathbf{x} \in [0, 1]^{m \times 1}. \end{aligned}$$

□

Applying Lemma A.5, we next prove Theorem 3.4. By using the result of Theorem 3.4, we show that the fairness-aware optimization problems, where the objective function includes both fairness (\mathcal{L}_{fair}) and accuracy (\mathcal{L}_{acc}) losses, can be transformed into linear programming (LP) problems.

THEOREM A.6 (RESTATED FROM THEOREM 3.4). *The fairness-aware optimization problems (Eqs. 2, 3, and 4) can be formulated as linear programming (LP) problems.*

PROOF. For every update of the model, the corresponding loss of each group can be approximated linearly in the same way as in Sec. A.2: $\tilde{\ell}(f_\theta, G) = \ell(f_\theta^{l-1}, G) - \eta \nabla_\theta \ell(f_\theta^{l-1}, G)^\top \nabla_\theta \ell(f_\theta^{l-1}, T_l)$. With a technique of sample weighting for the current task data, $\nabla_\theta \ell(f_\theta^{l-1}, T_l)$ can be changed as $\frac{1}{|T_l|} \sum_{d_i \in T_l} \mathbf{w}_i^l \nabla_\theta \ell(f_\theta^{l-1}, d_i)$ where \mathbf{w}_i^l represents a training weight for the current task sample d_i .

We believe that this transformation is natural and valid, as models are generally updated using the average gradient of training data, formulated as $\frac{1}{|T_l|} \sum_{d_i \in T_l} \nabla_\theta \ell(f_\theta^{l-1}, d_i)$, and a training weight is additionally assigned to each sample for weighting. Here, $|T_l|$ is the number of samples in the current task data, which is independent of the fairness notions considered. Note that if the normalization coefficient $\frac{1}{|T_l|}$ is replaced with $\frac{1}{\sum \mathbf{w}_i^l}$, the revised equation cannot handle the case where all weights are zero. Also, our revised optimization problems of Eqs. 2, 3, and 4 would no longer be LP. Thus, $\tilde{\ell}(f_\theta, G)$ can be rewritten as follows:

$$\begin{aligned} \tilde{\ell}(f_\theta, G) &= \ell(f_\theta^{l-1}, G) - \eta \nabla_\theta \ell(f_\theta^{l-1}, G)^\top \left(\frac{1}{|T_l|} \sum_{d_i \in T_l} \mathbf{w}_i^l \nabla_\theta \ell(f_\theta^{l-1}, d_i) \right) \\ &= \ell(f_\theta^{l-1}, G) - \frac{\eta}{|T_l|} \nabla_\theta \ell(f_\theta^{l-1}, G)^\top \langle [\dots, \nabla_\theta \ell(f_\theta^{l-1}, d_i), \dots] \\ & \quad , [\dots, \mathbf{w}_i^l, \dots]^\top \rangle \\ &= a_G - \mathbf{b}_G^\top \mathbf{w}, \end{aligned}$$

where $a_G := \ell(f_\theta^{l-1}, G)$ and $\mathbf{b}_G := \frac{\eta}{|T_l|} [\dots, \nabla_\theta \ell(f_\theta^{l-1}, d_i), \dots]^\top \cdot \nabla_\theta \ell(f_\theta^{l-1}, G)$ are a constant and a vector with constants, respectively, and $\mathbf{w} := [\dots, \mathbf{w}_i^l, \dots]^\top$ is a variable where $w_i^l \in [0, 1]$.

Case 1. If target fairness measure is EER ($\mathcal{L}_{fair} = \mathcal{L}_{EER}$),

$$\begin{aligned} & \mathcal{L}_{EER} + \lambda \mathcal{L}_{acc} \\ &= \frac{1}{|\mathbb{Y}|} \sum_{y \in \mathbb{Y}} |\tilde{\ell}(f_\theta, G_y) - \tilde{\ell}(f_\theta, G_{\mathbb{Y}})| + \lambda \frac{1}{|\mathbb{Y}_c|} \sum_{y \in \mathbb{Y}_c} \tilde{\ell}(f_\theta, G_y) \\ &= \frac{1}{|\mathbb{Y}|} \sum_{y \in \mathbb{Y}} |(a_{G_y} - a_{G_{\mathbb{Y}}}) - (\mathbf{b}_{G_y} - \mathbf{b}_{G_{\mathbb{Y}}})^\top \mathbf{w}| \\ & \quad + \lambda \frac{1}{|\mathbb{Y}_c|} \sum_{y \in \mathbb{Y}_c} (a_{G_y} - \mathbf{b}_{G_y}^\top \mathbf{w}). \end{aligned}$$

Case 2. If target fairness measure is EO ($\mathcal{L}_{fair} = \mathcal{L}_{EO}$),

$$\begin{aligned} & \mathcal{L}_{EO} + \lambda \mathcal{L}_{acc} \\ &= \frac{1}{|\mathbb{Y}| |\mathbb{Z}|} \sum_{y \in \mathbb{Y}, z \in \mathbb{Z}} |\tilde{\ell}(f_\theta, G_{y,z}) - \tilde{\ell}(f_\theta, G_y)| \\ & \quad + \lambda \frac{1}{|\mathbb{Y}_c| |\mathbb{Z}|} \sum_{y \in \mathbb{Y}_c, z \in \mathbb{Z}} \tilde{\ell}(f_\theta, G_{y,z}) \\ &= \frac{1}{|\mathbb{Y}| |\mathbb{Z}|} \sum_{y \in \mathbb{Y}, z \in \mathbb{Z}} |(a_{G_{y,z}} - a_{G_y}) - (\mathbf{b}_{G_{y,z}} - \mathbf{b}_{G_y})^\top \mathbf{w}| \\ & \quad + \lambda \frac{1}{|\mathbb{Y}_c| |\mathbb{Z}|} \sum_{y \in \mathbb{Y}_c, z \in \mathbb{Z}} (a_{G_{y,z}} - \mathbf{b}_{G_{y,z}}^\top \mathbf{w}). \end{aligned}$$

Case 3. If target fairness measure is DP ($\mathcal{L}_{fair} = \mathcal{L}_{DP}$),

$$\begin{aligned} & \mathcal{L}_{DP} + \lambda \mathcal{L}_{acc} \\ &= \frac{1}{|\mathbb{Y}| |\mathbb{Z}|} \sum_{y \in \mathbb{Y}, z \in \mathbb{Z}} |\tilde{\ell}'(f_\theta, G_{y,z}) - \tilde{\ell}'(f_\theta, G_y)| \\ & \quad + \lambda \frac{1}{|\mathbb{Y}_c| |\mathbb{Z}|} \sum_{y \in \mathbb{Y}_c, z \in \mathbb{Z}} \tilde{\ell}'(f_\theta, G_{y,z}) \\ &= \frac{1}{|\mathbb{Y}| |\mathbb{Z}|} \sum_{y \in \mathbb{Y}, z \in \mathbb{Z}} |(a'_{G_{y,z}} - a'_{G_y}) - (\mathbf{b}'_{G_{y,z}} - \mathbf{b}'_{G_y})^\top \mathbf{w}| \\ & \quad + \lambda \frac{1}{|\mathbb{Y}_c| |\mathbb{Z}|} \sum_{y \in \mathbb{Y}_c, z \in \mathbb{Z}} (a_{G_{y,z}} - \mathbf{b}_{G_{y,z}}^\top \mathbf{w}), \end{aligned}$$

where $a'_{G_{y,z}} := \frac{m_{y,z}}{m_{*,z}} a_{G_{y,z}}$, $a'_{G_y} := \sum_{z \in \mathbb{Z}} \frac{m_{y,z}}{m_{*,z}} a_{G_{y,z}}$, $\mathbf{b}'_{G_{y,z}} := \frac{m_{y,z}}{m_{*,z}} \mathbf{b}_{G_{y,z}}$, $\mathbf{b}'_{G_y} := \sum_{z \in \mathbb{Z}} \frac{m_{y,z}}{m_{*,z}} \mathbf{b}_{G_{y,z}}$.

Since a_G and \mathbf{b}_G are composed of constant values, each equation above can be reformulated to a linear programming form by applying Lemma A.5. □

Remark (Non-triviality of the solution). Although the weights w_I are constrained to $[0, 1]^{|T_I|}$, the optimization does not admit the trivial solution $\mathbf{w} = \mathbf{0}$ unless $\lambda = 0$. This is because the objective jointly optimizes both accuracy and fairness objectives: assigning zero weights eliminates the fairness term, while the prediction loss reduces to a constant term (the a_G terms).

Remark (Generality of the fairness formulation). Although we focus on EER, EO, and DP in this work, the formulation in Sec. A.6 is not restricted to these specific metrics. More generally, any group fairness notion that can be expressed as a function of group-wise performance disparities admits a similar LP formulation, and can therefore be incorporated into our framework.

B More Experimental Results

B.1 T-SNE Results for Real Datasets

Continuing from Sec. 1, we provide t-SNE results for real datasets to show that data overlapping between different classes also occurs in real scenarios, similar to the synthetic dataset results depicted in Fig. 1a. Using t-SNE, we project the high-dimensional data of the MNIST, FMNIST, Biased MNIST, and DRUG datasets into a lower-dimensional 2D space with x_1 and x_2 , as shown in Fig. 5. Since BiasBios is a text dataset that requires pre-trained embeddings to represent the data, we do not include the t-SNE results for it. In the MNIST dataset, the images with labels of 3 (red), 5 (brown), and 8 (yellow) exhibit similar characteristics and overlap, but belong to different classes. As another example, in the FMNIST dataset, the images of the classes ‘Sandal’ (brown), ‘Sneaker’ (gray), and ‘Ankel boot’ (sky-blue) also have similar characteristics and overlap.

B.2 Approximation Error of Taylor Series

Continuing from Sec. 3.1, we provide empirical approximation errors between true losses and approximated losses derived from first-order Taylor series on the MNIST and Biased MNIST datasets as shown in Fig. 6. For each task, we train the model for 5 epochs and 15 epochs on the MNIST and Biased MNIST datasets, respectively. The approximation error is large when a new task begins because new samples with unseen classes are introduced. However, the error gradually decreases as the number of epochs increases while training a model for the task.

B.3 Computational Complexity and Runtime Results of FSW

Continuing from Sec. 3.3, we provide computational complexity as shown in Fig. 7. Our empirical results show that for about twelve thousand current-task samples, the time to solve an LP problem is a few seconds for the MNIST dataset. By applying the log-log regression model to the results in Fig. 7, the computational complexity of solving LP at each epoch is $O(|T_i|^{1.642})$ where $|T_i|$ denotes the number of current task samples. We note that this complexity can be quadratic in the worst case. If the task size becomes too large, we believe that clustering similar samples and assigning weights to the clusters, rather than samples, could be a solution to reduce the computational overhead. A more detailed discussion is provided in Sec. D.2.

We also show overall runtime results of FSW using the MNIST and Biased MNIST datasets and compare the total runtime of all baselines in Fig. 8 and Table 8, respectively. In Fig. 8, we present the overall runtime of FSW divided into three steps: Gradient Computation, CPLEX Computation, and Model Training. The total runtime of FSW with other baselines is in Table 8, and we checked that the overhead of FSW is not excessive compared to the baselines.

Table 8: Overall runtime results of FSW (w.r.t. EO Disp.) with other baselines on the Biased MNIST datasets.

Methods	FSW	iCaRL	WA	CLAD	GSS	OCS	FaIRL
Time (sec)	835±018	947±015	177±023	96±018	5563±069	2681±074	5827±228

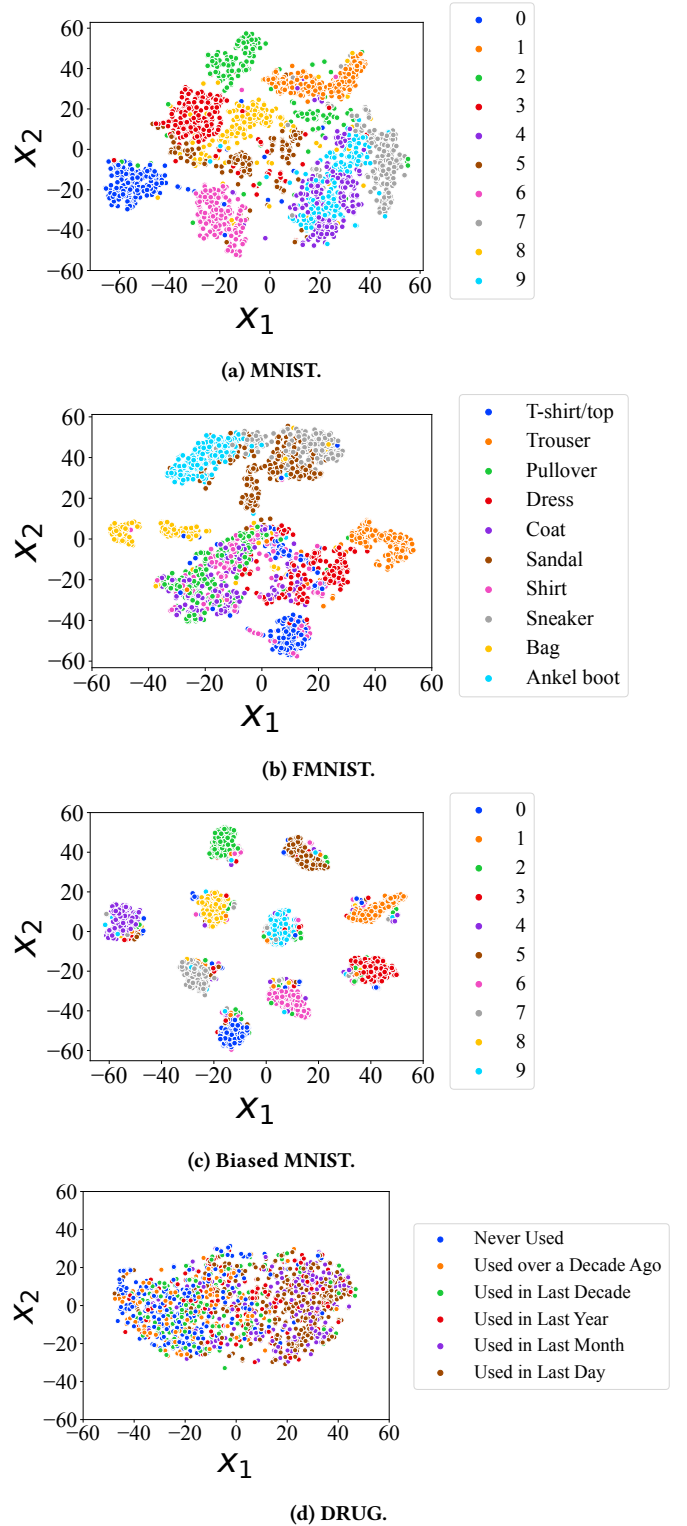
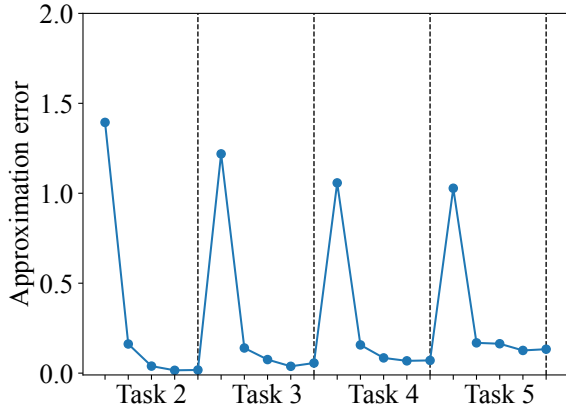
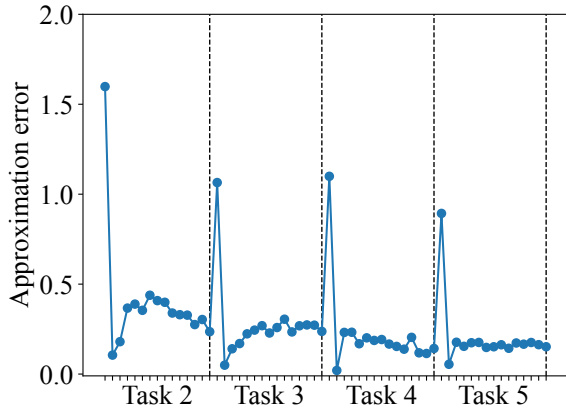


Figure 5: t-SNE results for the MNIST, FMNIST, Biased MNIST, and DRUG datasets.



(a) MNIST.



(b) Biased MNIST.

Figure 6: Absolute errors between true losses and approximated losses derived from first-order Taylor series while training a model.

B.4 More Details on Datasets

Continuing from Sec. 4.1.2, we provide more details of the two datasets using the class as the sensitive attribute and the three datasets with separate sensitive attributes. For datasets with a total of C classes, we divide the datasets into L sequences of tasks where each task consists of C/L classes, and assume that task boundaries are available [82]. We also consider using standard benchmark datasets in the fairness field, but they are unsuitable for class-incremental learning experiments either because there are only two classes (e.g., COMPAS [6], AdultCensus [52], and Jigsaw [24]), or because it is difficult to apply group fairness metrics. For instance, in the case of CelebA [57], each person is considered a class, making the sensitive attribute dependent on the true label.

MNIST [54]. The MNIST dataset is a standard benchmark for evaluating the performance of machine learning models, especially in image classification tasks. The dataset is a collection of grayscale images of handwritten digits ranging from 0 to 9, each measuring 28 pixels in width and 28 pixels in height. The dataset consists of

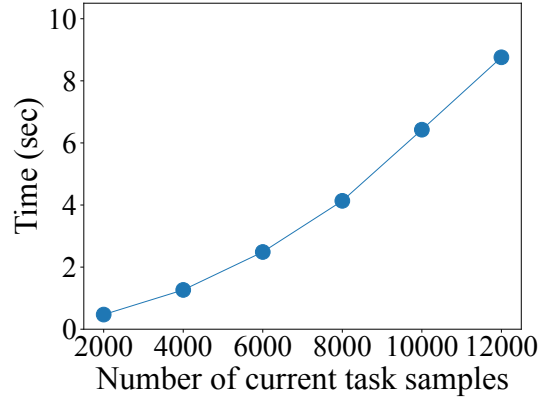


Figure 7: Runtime results of solving a single LP problem in FSW using CPLEX for the MNIST dataset.

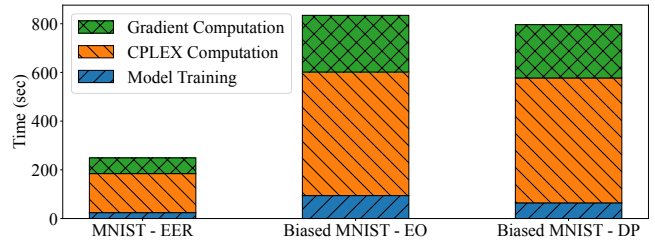


Figure 8: Overall runtime results of our framework on all tasks for three datasets: MNIST-EER, Biased MNIST-EO, and Biased MNIST-DP.

60,000 training images and 10,000 test images. We configure a class-incremental learning setup, where a total of 10 classes are evenly distributed across 5 tasks, with 2 classes per task. We assume the class itself is the sensitive attribute.

Fashion-MNIST (FMNIST) [87]. The Fashion-MNIST dataset is a specialized variant of the original MNIST dataset, designed for the classification of various clothing items into 10 distinct classes. The classes include ‘T-shirt/top’, ‘Trouser’, ‘Pullover’, ‘Dress’, ‘Coat’, ‘Sandal’, ‘Shirt’, ‘Sneaker’, ‘Bag’, and ‘Ankle boot’. The dataset consists of grayscale images with dimensions of 28 pixels by 28 pixels including 60,000 training images and 10,000 test images. We configure a class-incremental learning setup, where a total of 10 classes are evenly distributed across 5 tasks, with 2 classes per task. We assume the class itself is the sensitive attribute.

Biased MNIST [10]. The Biased MNIST dataset is a modified version of the MNIST dataset that introduces bias by incorporating background colors highly correlated with the digits. We select 10 distinct background colors and assign one to each digit from 0 to 9. For the training images, each digit is assigned the selected background color with a probability of 0.95, or one of the other colors at random with a probability of 0.05. For the test images, the background color of each digit is assigned from the selected color or other random colors with equal probability of 0.5. The dataset consists of 60,000 training images and 10,000 test images.

We configure a class-incremental learning setup, where a total of 10 classes are evenly distributed across 5 tasks, with 2 classes per task. We set the background color as the sensitive attribute and consider two sensitive groups: the origin color and other random colors for each digit.

Drug Consumption (DRUG) [32]. The Drug Consumption dataset contains information about the usage of various drugs by individuals and correlates it with different demographic and personality traits. The dataset includes records for 1,885 respondents, each with 12 attributes including NEO-FFI-R, BIS-11, ImpSS, level of education, age, gender, country of residence, and ethnicity. We split the dataset into the ratio of 70/30 for training and testing. All input attributes are originally categorical, but we quantify them as real values for training. Participants were questioned about their use of 18 drugs, and our task is to predict cannabis usage. The label variable contains six classes: ‘Never Used’, ‘Used over a Decade Ago’, ‘Used in Last Decade’, ‘Used in Last Year’, ‘Used in Last Month’, and ‘Used in Last Day’. We configure a class-incremental learning setup, where a total of 6 classes are distributed across 3 tasks, with 2 classes per task. We set gender as the sensitive attribute and consider two sensitive groups: male and female.

BiasBios [27]. The BiasBios dataset is a benchmark designed to explore and evaluate bias in natural language processing models, particularly in the context of profession classification from bios. The dataset consists of short textual biographies collected from online sources, labeled with one of the 28 profession classes, such as ‘professor’, ‘nurse’, or ‘software engineer’. The dataset includes gender annotations, which makes it suitable for studying biases related to gender. The dataset contains approximately 350k biographies where 253k are for training and 97k for testing. We configure a class-incremental learning setup using the 25 most-frequent professions, where a total of 25 classes are distributed across 5 tasks, with 5 classes per task. As the number of samples for each class varies significantly, we arrange the classes in descending order based on their size [21]. We set gender as the sensitive attribute and consider two sensitive groups: male and female.

B.5 More Details on Models and Hyperparameters

Continuing from Sec. 4.1.3, we provide more details on experimental settings. For training, we use an SGD optimizer with momentum 0.9 and a batch size of 64 for all experiments. We also set the initial learning rate and the number of epochs for each dataset as follows: For the MNIST, FMNIST, Biased MNIST, and DRUG datasets, we train both our model and baselines with initial learning rates of [0.001, 0.01, 0.1], for 5, 5, 15, and 25 epochs, respectively. For the BiasBios dataset, we use learning rates of [0.00002, 0.0001, 0.001] for 10 epochs and set the maximum token length to 128. For hyperparameters, we perform cross-validation with a grid search for $\alpha \in \{0.0005, 0.001, 0.002, 0.01\}$, $\lambda \in \{0.1, 0.5, 1\}$, and $\tau \in \{1, 2, 5, 10\}$. All evaluations are performed on separate test sets and repeated with five random seeds. We write the average and standard deviation of performance results and run experiments on Intel Xeon Silver 4114 CPUs and NVIDIA RTX A6000 GPUs.

B.6 More Results on Accuracy and Fairness

Continuing from Sec. 4.2, we compare FSW with other baselines with respect to EER, EO, and DP disparity as shown in Tables 9, 10, and 11, respectively.

On BiasBios, *iCaRL*’s accuracy surpasses even *Joint training*, commonly considered the upper bound, while it has low accuracy on the Biased MNIST dataset. *iCaRL*’s high accuracy on BiasBios likely stems from its prototypical classifier, which is structurally distinct from the fully-connected layer used by other methods. On the other hand, FSW achieves fairness and accuracy comparable to *Joint training* on BiasBios, effectively mitigating unfair forgetting without compromising accuracy. As illustrated by the t-SNE visualization on the Biased MNIST dataset (Sec. B.1), some samples are misaligned due to background color biases, causing difficulty for *iCaRL* to accurately classify these points. In comparison, FSW consistently exhibits lower EO and DP disparities compared to *iCaRL* for all the datasets. This supports that FSW is more robust, particularly when the backbone network struggles to generate discriminative representations.

We note that the performance of *FaIRL* in our experiments may not fully represent its potential. However, the complicated model structure of *FaIRL* not only causes the instability of training, but also introduces additional multiple loss terms, resulting in numerous hyperparameters that are difficult to optimize. Using the identical hyperparameter set from *FaIRL* shows significantly lower performance, mainly because we standardize all models to use the same backbone for a fair comparison, differing from *FaIRL*’s original setup. Moreover, among all the baseline methods, *FaIRL* requires the longest training time, as discussed in Sec B.3, limiting our ability to thoroughly tune its hyperparameters. Consequently, the inherent challenges of the method and experimental constraints lead to suboptimal results.

B.7 More Results on Tradeoff between Accuracy and Fairness

Continuing from Sec. 4.2, we evaluate the tradeoff between accuracy and fairness of FSW with other baselines as shown in Fig. 9–Fig. 12. The figures show FSW positioned in the lower right corner of the graph, indicating better accuracy-fairness tradeoff results compared to other baselines. FSW in the figures represents the result for different values of λ , a hyperparameter that balances fairness and accuracy. Since other baselines do not have a balancing parameter, we select Pareto-optimal points from all search spaces, where a Pareto-optimal point is defined as a point for which there does not exist another point with both higher accuracy and lower fairness disparity.

B.8 More Results on Sequential Accuracy and Fairness

Continuing from Sec. 4.2, we present the sequential performance results for each task as shown in Fig. 13–Fig. 20.

Table 9: Accuracy and fairness results on the MNIST and FMNIST datasets with respect to EER disparity, where the class is the sensitive attribute. We compare FSW with four types of baselines: naïve (Joint Training and Fine Tuning), state-of-the-art (iCaRL, WA, and CLAD), sample selection (GSS and OCS), and fairness-aware (FaIRL) methods. We mark the best and second-best results with bold and underline, respectively.

Methods	MNIST		FMNIST	
	Acc.	EER Disp.	Acc.	EER Disp.
Joint Training	.989 \pm .000	.003 \pm .000	.921 \pm .002	.024 \pm .002
Fine Tuning	.455 \pm .000	.326 \pm .000	.451 \pm .000	.325 \pm .000
iCaRL	.918 \pm .005	.048 \pm .003	.852\pm.002	<u>.047\pm.001</u>
WA	.911 \pm .007	.052 \pm .006	.809 \pm .005	.088 \pm .003
CLAD	.835 \pm .016	.099 \pm .016	.782 \pm .018	.118 \pm .022
GSS	.889 \pm .010	.080 \pm .009	.732 \pm .021	.149 \pm .019
OCS	.929\pm.002	<u>.040\pm.003</u>	.799 \pm .008	.109 \pm .007
FaIRL	.558 \pm .060	.273 \pm .018	.531 \pm .032	.289 \pm .019
FSW	<u>.925\pm.004</u>	.032\pm.005	<u>.824\pm.006</u>	.039\pm.006

Table 10: Accuracy and fairness results on the Biased MNIST, DRUG, and BiasBios datasets with respect to EO disparity, where background color is the sensitive attribute for Biased MNIST, and gender for DRUG and BiasBios, respectively. Due to the excessive time (>5 days) required to run OCS on BiasBios, we are not able to measure the results and mark them as ‘-’. The other settings are the same as in Table 9.

Methods	Biased MNIST		DRUG		BiasBios	
	Acc.	EO Disp.	Acc.	EO Disp.	Acc.	EO Disp.
Joint Training	.944 \pm .002	.108 \pm .003	.442 \pm .015	.179 \pm .052	.823 \pm .002	.076 \pm .001
Fine Tuning	.449 \pm .001	.016 \pm .002	.357 \pm .009	.125 \pm .034	.420 \pm .001	.028 \pm .002
iCaRL	.802 \pm .008	.365 \pm .021	.444\pm.025	.190 \pm .017	.829\pm.002	.084 \pm .003
WA	.916\pm.002	.140 \pm .004	.408 \pm .022	.134 \pm .029	.796 \pm .003	.076 \pm .001
CLAD	.871 \pm .012	.198 \pm .022	.410 \pm .026	.114 \pm .043	.799 \pm .003	.074 \pm .002
GSS	.809 \pm .005	.325 \pm .017	<u>.426\pm.010</u>	.167 \pm .038	<u>.808\pm.003</u>	.081 \pm .002
OCS	.824 \pm .007	.331 \pm .013	.406 \pm .024	.142 \pm .030	-	-
FaIRL	.411 \pm .012	.118\pm.011	.354 \pm .011	.060\pm.021	.400 \pm .060	.055\pm.020
FSW	<u>.909\pm.004</u>	<u>.119\pm.007</u>	.406 \pm .014	<u>.077\pm.010</u>	<u>.808\pm.002</u>	<u>.072\pm.001</u>

Table 11: Accuracy and fairness results on the Biased MNIST, DRUG, and BiasBios datasets with respect to DP disparity. The other settings are the same as in Table 10.

Methods	Biased MNIST		DRUG		BiasBios	
	Acc.	DP Disp.	Acc.	DP Disp.	Acc.	DP Disp.
Joint Training	.944 \pm .002	.006 \pm .001	.442 \pm .015	.090 \pm .020	.823 \pm .002	.021 \pm .000
Fine Tuning	.449 \pm .001	.017 \pm .008	.357 \pm .009	.102 \pm .013	.420 \pm .001	.028 \pm .002
iCaRL	.802 \pm .008	.015 \pm .001	.444\pm.025	.093 \pm .009	.829\pm.002	<u>.022\pm.000</u>
WA	.916\pm.002	<u>.009\pm.001</u>	.408 \pm .022	.067 \pm .013	.796 \pm .003	<u>.022\pm.000</u>
CLAD	.871 \pm .012	.013 \pm .001	<u>.410\pm.026</u>	.069 \pm .019	.799 \pm .003	<u>.022\pm.000</u>
GSS	.809 \pm .005	.039 \pm .003	.392 \pm .022	.065 \pm .015	.808 \pm .003	.023 \pm .000
OCS	.824 \pm .007	.035 \pm .003	.393 \pm .017	.053 \pm .012	-	-
FaIRL	.411 \pm .012	.026 \pm .008	.354 \pm .011	.040\pm.008	.400 \pm .060	.015\pm.002
FSW	<u>.904\pm.004</u>	.008\pm.001	.405 \pm .013	<u>.043\pm.004</u>	<u>.809\pm.003</u>	<u>.022\pm.000</u>

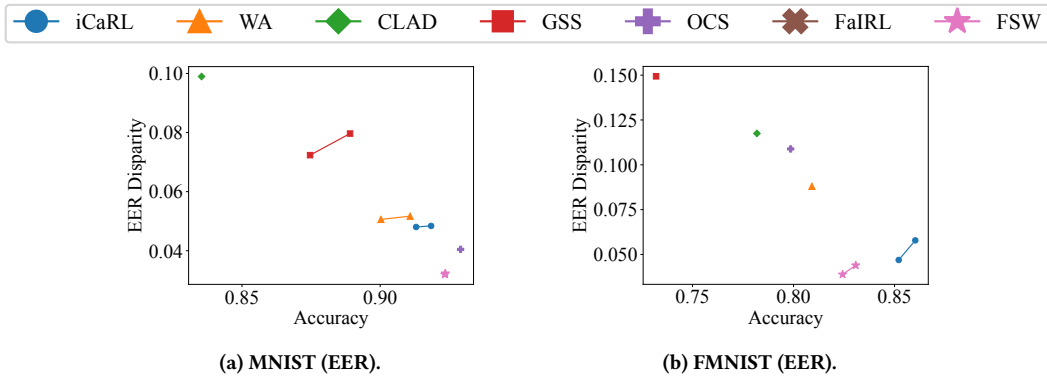


Figure 9: Tradeoff results between accuracy and fairness (EER) on the MNIST and FMNIST datasets.

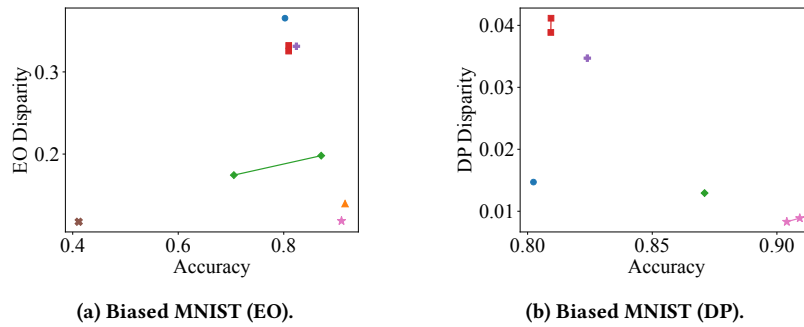


Figure 10: Tradeoff results between accuracy and fairness (EO and DP) on the Biased MNIST dataset.

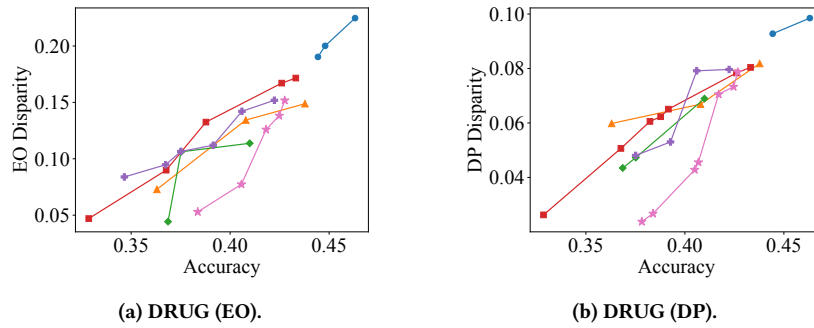


Figure 11: Tradeoff results between accuracy and fairness (EO and DP) on the DRUG dataset.

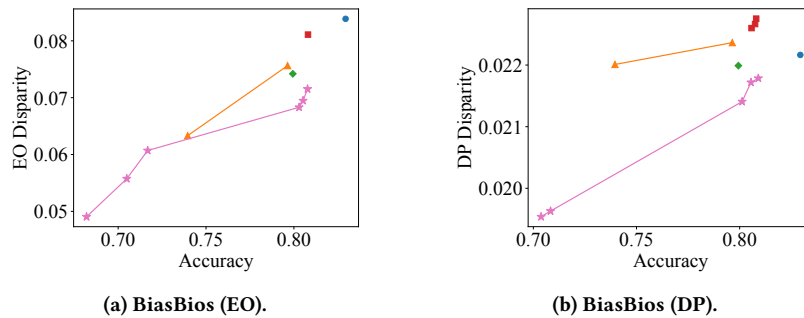


Figure 12: Tradeoff results between accuracy and fairness (EO and DP) on the BiasBios dataset.

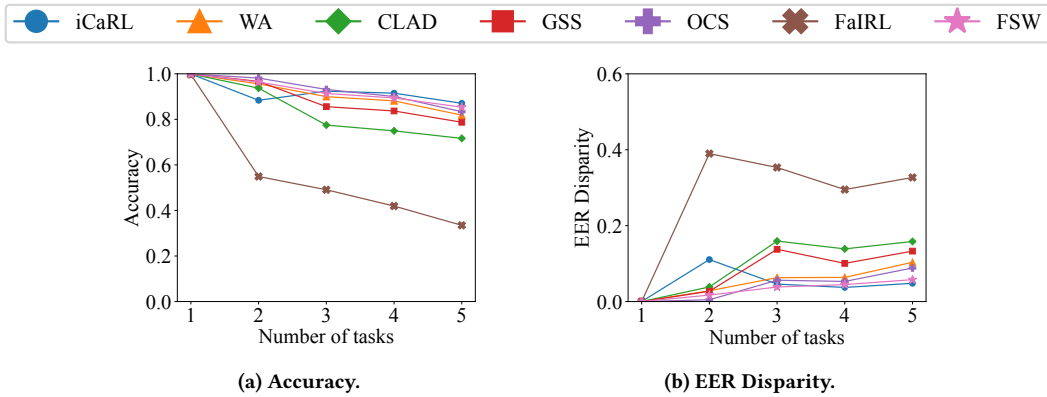


Figure 13: Sequential accuracy and fairness (EER) results on the MNIST dataset.

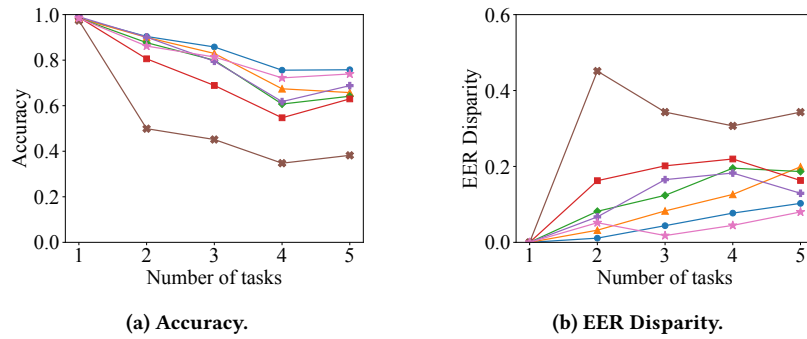


Figure 14: Sequential accuracy and fairness (EER) results on the FMNIST dataset.

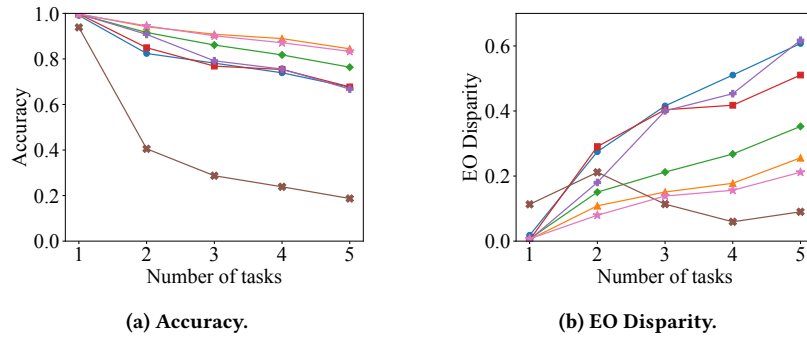


Figure 15: Sequential accuracy and fairness (EO) results on the Biased MNIST dataset.

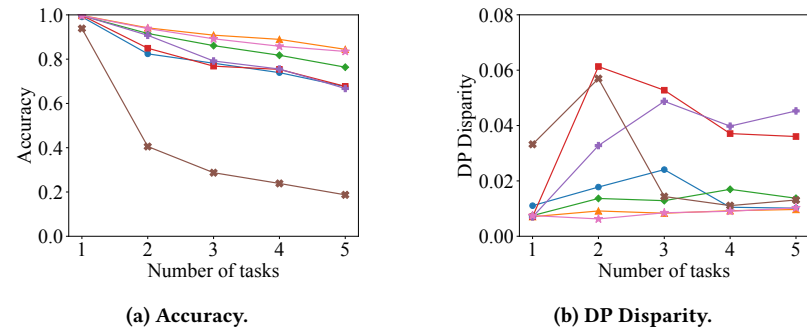
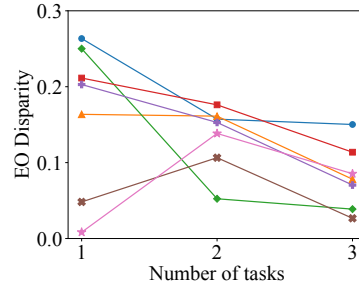
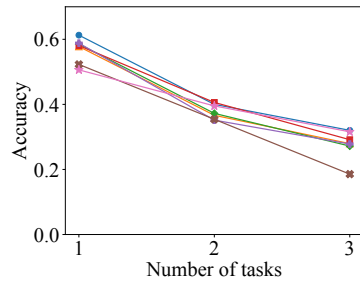


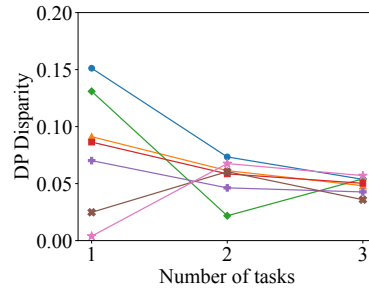
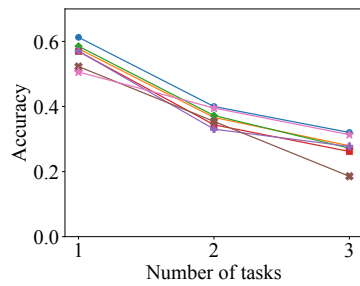
Figure 16: Sequential accuracy and fairness (DP) results on the Biased MNIST dataset.



(a) Accuracy.

(b) EO Disparity.

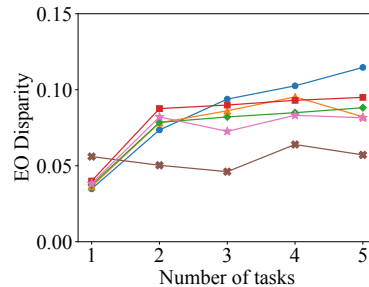
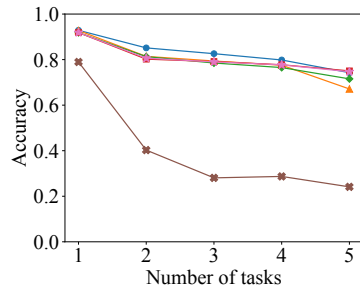
Figure 17: Sequential accuracy and fairness (EO) results on the DRUG dataset.



(a) Accuracy.

(b) DP Disparity.

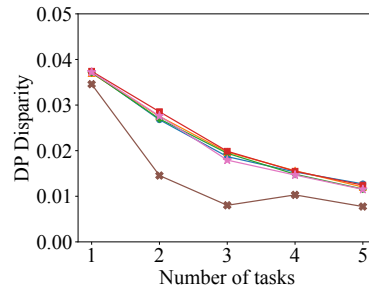
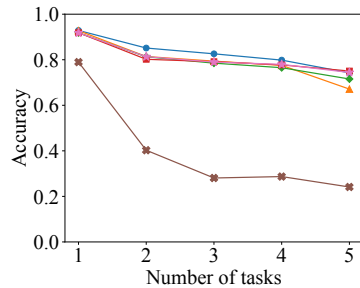
Figure 18: Sequential accuracy and fairness (DP) results on the DRUG dataset.



(a) Accuracy.

(b) EO Disparity.

Figure 19: Sequential accuracy and fairness (EO) results on the BiasBios dataset.



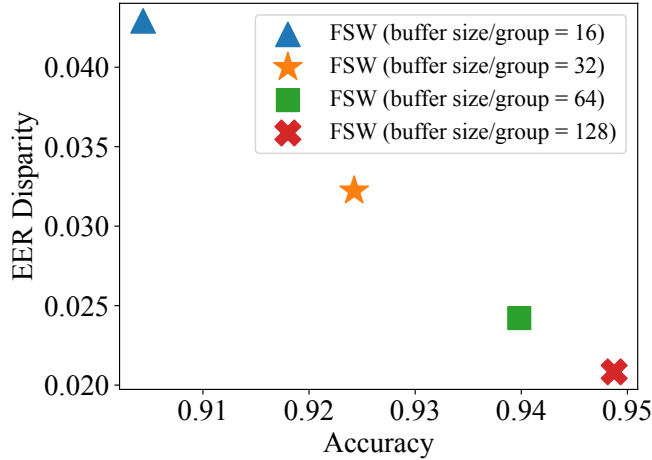
(a) Accuracy.

(b) DP Disparity.

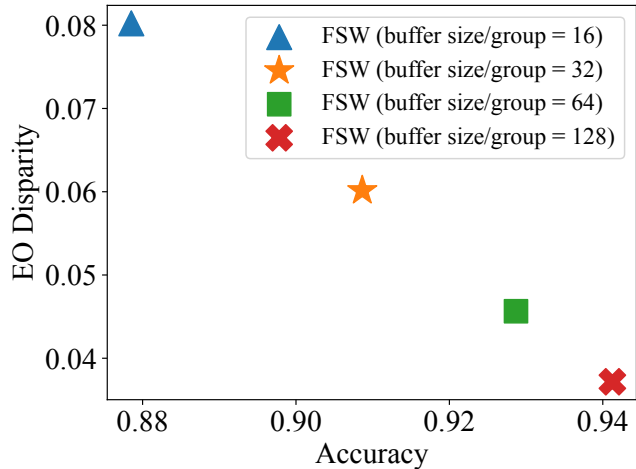
Figure 20: Sequential accuracy and fairness (DP) results on the BiasBios dataset.

B.9 More Results of FSW when Varying the Buffer Size

Continuing from Sec. 4.2, we have additional experimental results of FSW on the MNIST and Biased MNIST datasets when varying the buffer size to 16, 32, 64, and 128 per sensitive group as shown in Fig. 21. As the buffer size increases, both accuracy and fairness performances improve. In addition, we compute the number of current task data assigned with non-zero weights as shown in Fig. 22, and there is no clear relationship between the buffer size and weights.

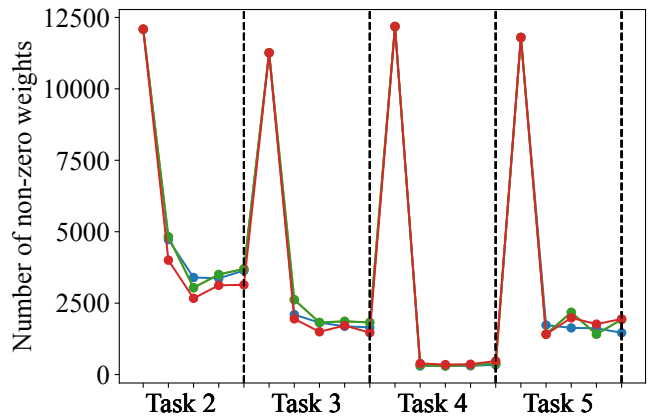


(a) MNIST.

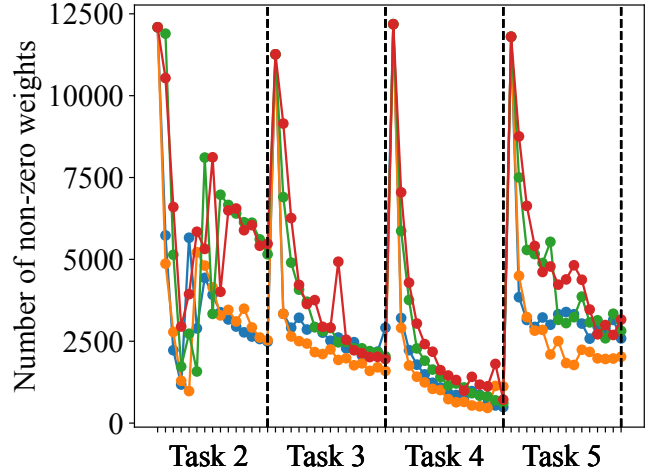


(b) Biased MNIST.

Figure 21: Accuracy and fairness results of FSW when varying the buffer size on the MNIST and Biased MNIST datasets.



(a) MNIST.



(b) Biased MNIST.

Figure 22: Number of current task data assigned with non-zero weights when varying the buffer size on the MNIST and Biased MNIST datasets.

B.10 More Results on Sample Weighting Analysis

Continuing from Sec. 4.3, we show more results from the sample weighting analysis for all sequential tasks of each dataset, as shown in the figures below (Fig. 23–Fig. 30).

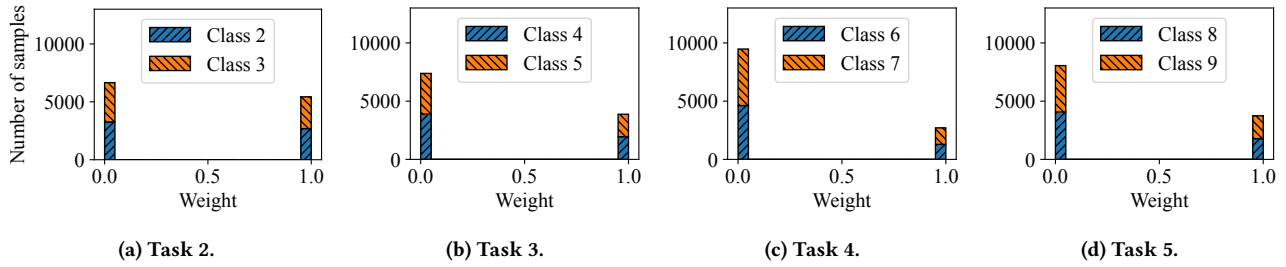


Figure 23: Distribution of sample weights for EER in sequential tasks of the MNIST dataset.

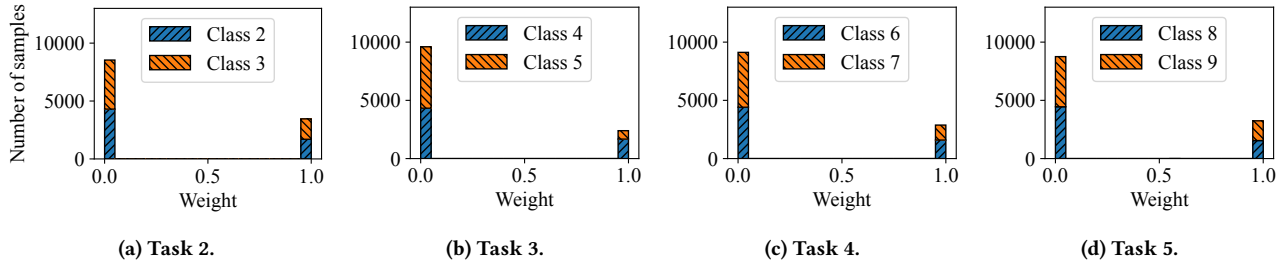


Figure 24: Distribution of sample weights for EER in sequential tasks of the FMNIST dataset.

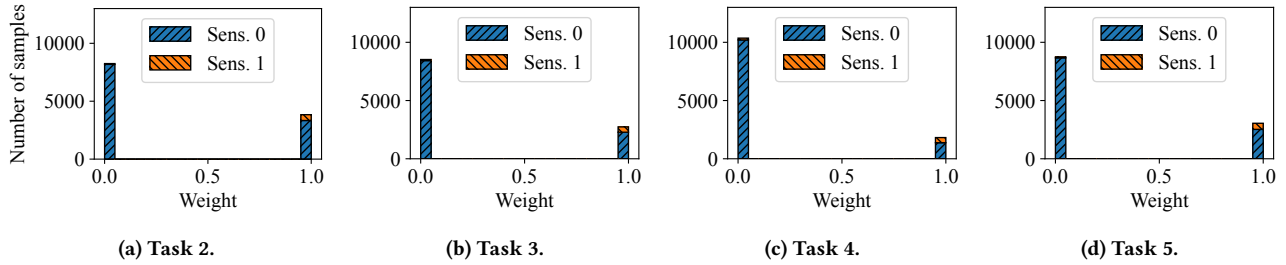


Figure 25: Distribution of sample weights for EO in sequential tasks of the Biased MNIST dataset.

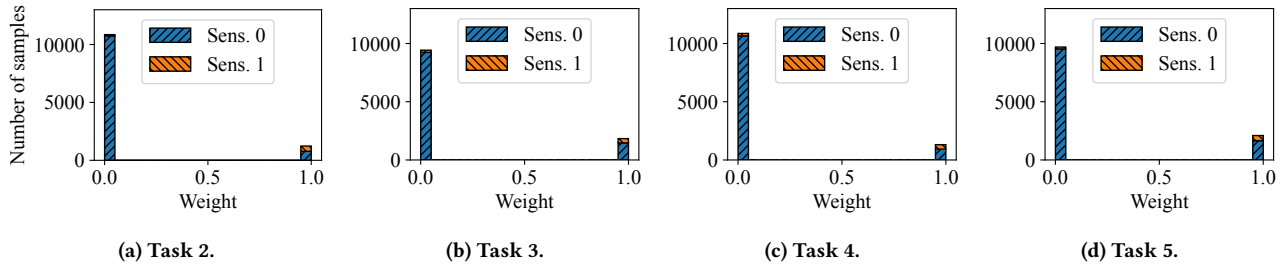


Figure 26: Distribution of sample weights for DP in sequential tasks of the Biased MNIST dataset.

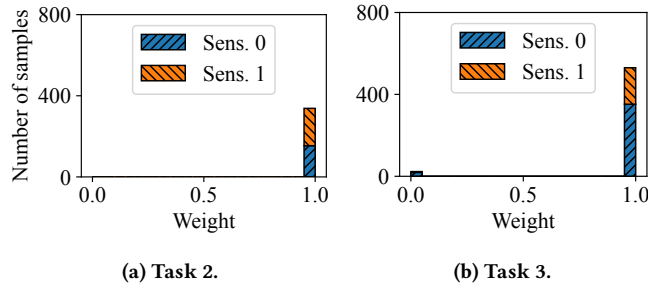


Figure 27: Distribution of sample weights for EO in sequential tasks of the DRUG dataset.

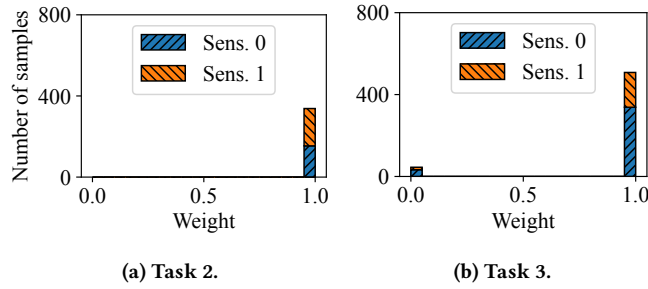


Figure 28: Distribution of sample weights for DP in sequential tasks of the DRUG dataset.

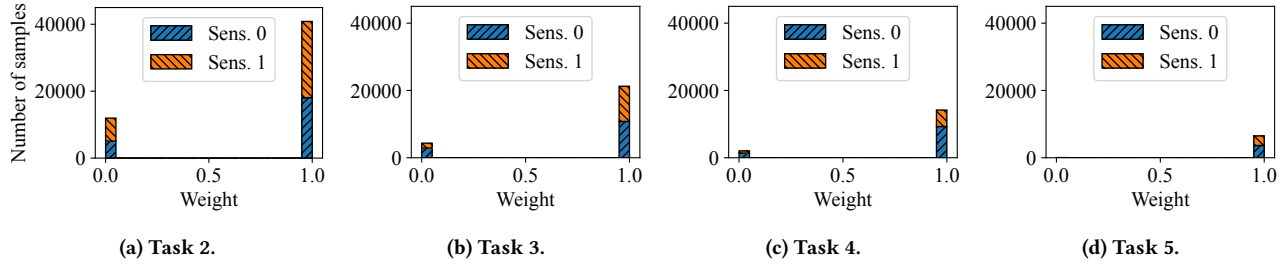


Figure 29: Distribution of sample weights for EO in sequential tasks of the BiasBios dataset.

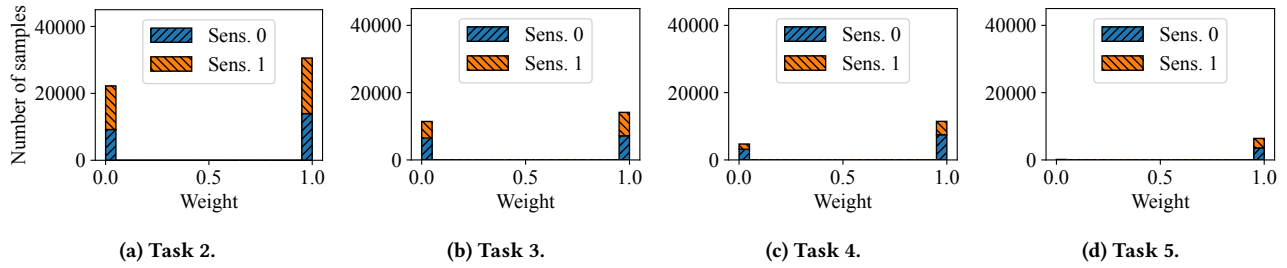


Figure 30: Distribution of sample weights for DP in sequential tasks of the BiasBios dataset.

B.11 More Results on Ablation Study

Continuing from Sec. 4.4, we present additional results of the ablation study to demonstrate the contribution of FSW to the overall accuracy and fairness performance. The results are shown in Tables 12, 13, and 14.

Table 12: Accuracy and fairness results on the MNIST and FMNIST datasets, with respect to EER disparity with or without FSW.

Methods	MNIST		FMNIST	
	Acc.	EER Disp.	Acc.	EER Disp.
W/o FSW	.912 \pm .004	.051 \pm .005	.810 \pm .004	.092 \pm .003
FSW	.925\pm.004	.032\pm.005	.824\pm.006	.039\pm.006

Table 13: Accuracy and fairness results on the Biased MNIST, DRUG, and BiasBios datasets with respect to EO disparity with or without FSW.

Methods	Biased MNIST		DRUG		BiasBios	
	Acc.	EO Disp.	Acc.	EO Disp.	Acc.	EO Disp.
W/o FSW	.910 \pm .003	.126 \pm .005	.402 \pm .010	.080 \pm .005	.806 \pm .003	.073 \pm .002
FSW	.909\pm.004	.119\pm.007	.406\pm.014	.077\pm.010	.808\pm.002	.072\pm.001

Table 14: Accuracy and fairness results on the Biased MNIST, DRUG, and BiasBios datasets with respect to DP disparity with or without FSW.

Methods	Biased MNIST		DRUG		BiasBios	
	Acc.	DP Disp.	Acc.	DP Disp.	Acc.	DP Disp.
W/o FSW	.910 \pm .003	.009 \pm .001	.402 \pm .010	.044 \pm .004	.806 \pm .003	.022 \pm .000
FSW	.904\pm.004	.008\pm.001	.405\pm.013	.043\pm.004	.809\pm.003	.022\pm.000

B.12 Impact on Non-targeted Fairness Metrics

Continuing from Sec. 4.4, we further investigate the effect of optimizing FSW for a specific fairness metric on other non-targeted fairness metrics. The results are shown in Tables 15, 16, and 17.

Table 15: Accuracy and more fairness metrics (including EO, DP, and EER Disparity) results on the Biased MNIST dataset without FSW, FSW with respect to EO and DP disparity.

Methods	Acc.	EO Disp.	DP Disp.	EER Disp.
W/o FSW	.910 \pm .003	.126 \pm .005	.009 \pm .001	.032 \pm .002
FSW (w.r.t. EO Disp.)	.909 \pm .004	.119\pm.007	.008\pm.001	.032 \pm .003
FSW (w.r.t. DP Disp.)	.904 \pm .004	.124 \pm .008	.008\pm.001	.029\pm.004

Table 16: Accuracy and more fairness metrics (including EO, DP, and EER Disparity) results on the DRUG dataset without FSW, FSW with respect to EO and DP disparity.

Methods	Acc.	EO Disp.	DP Disp.	EER Disp.
W/o FSW	.402 \pm .010	.080 \pm .005	.044 \pm .004	.078 \pm .008
FSW (w.r.t. EO Disp.)	.406\pm.014	.077\pm.010	.043\pm.004	.077\pm.007
FSW (w.r.t. DP Disp.)	.405 \pm .013	.079 \pm .006	.043\pm.004	.078 \pm .006

Table 17: Accuracy and more fairness metrics (including EO, DP, and EER Disparity) results on the BiasBios dataset without FSW, FSW with respect to EO and DP disparity.

Methods	Acc.	EO Disp.	DP Disp.	EER Disp.
W/o FSW	.806 \pm .003	.073 \pm .002	.022\pm.000	.056 \pm .002
FSW (w.r.t. EO Disp.)	.808 \pm .002	.072 \pm .001	.022\pm.000	.049 \pm .005
FSW (w.r.t. DP Disp.)	.809\pm.003	.069\pm.002	.022\pm.000	.036\pm.009

B.13 More Results on Integrating FSW with a Fair Post-processing Method

Continuing from Sec. 4.5, we provide additional results on integrating with a fair post-processing method (ϵ -fair) as shown in Table 18.

B.14 Alternative Loss Function for Group Fairness Metrics

Continuing from Sec. 3.1, we use cross-entropy loss disparity to approximate group fairness metrics such as EER, EO, and DP disparity. Both theoretical and empirical results show that the cross-entropy loss disparity can effectively approximate these group fairness metrics, as discussed in Sec. A.4. However, the cross-entropy loss disparity is not the only possible type of loss for approximating the group fairness metrics; the disparity of other loss functions may yield better performance. Our method can be applied regardless of the loss definition if (1) the loss update process can be linearly approximated (as in Sec. A.2) and (2) the loss disparity promotes fairness (as in Sec. A.4).

To verify if FSW can also be effective with different loss function designs, we conduct simple experiments using hinge loss (i.e., $\sum_{j \neq y_i} \max(0, s_j - s_{y_i} + 1)$ where y_i is the true label, and s_j is the softmax output for label j) to approximate group fairness metrics in FSW. The results are shown in Tables 19, 20, and 21. Overall, both methods show comparable accuracy-fairness results, suggesting that FSW performs well regardless of the type of loss function used to approximate group fairness metrics. Here, we would like to note that the cross-entropy loss disparity is widely used and empirically verified as a reasonable proxy for capturing group fairness metrics [37, 75, 76, 78], which is why we use it, although we could also use other losses.

Table 18: Accuracy and fairness (DP disparity) results when combining fair post-processing techniques (ϵ -fair) with continual learning methods (iCaRL, WA, CLAD, GSS, OCS, and FSW). Due to the excessive time (>5 days) required to run OCS on BiasBios, we are not able to measure the results and mark them as ‘-’.

Methods	Biased MNIST		DRUG		BiasBios	
	Acc.	DP Disp.	Acc.	DP Disp.	Acc.	DP Disp.
iCaRL	.802 \pm .008	.015 \pm .001	.444 \pm .025	.093 \pm .009	.829 \pm .002	.022 \pm .000
WA	.916 \pm .002	.009 \pm .001	.408 \pm .022	.067 \pm .013	.796 \pm .003	.022 \pm .000
CLAD	.871 \pm .012	.013 \pm .001	.410 \pm .026	.069 \pm .019	.799 \pm .003	.022 \pm .000
GSS	.809 \pm .005	.039 \pm .003	.392 \pm .022	.065 \pm .015	.808 \pm .003	.023 \pm .000
OCS	.824 \pm .007	.035 \pm .003	.393 \pm .017	.053 \pm .012	-	-
FSW	.904 \pm .004	.008 \pm .001	.405 \pm .013	.043 \pm .004	<u>.809</u> \pm .003	.022 \pm .000
iCaRL - ϵ -fair	.944 \pm .008	<u>.006</u> \pm .002	<u>.427</u> \pm .018	<u>.026</u> \pm .004	.753 \pm .002	<u>.017</u> \pm .000
WA - ϵ -fair	.953 \pm .003	<u>.006</u> \pm .002	.404 \pm .021	.044 \pm .020	.708 \pm .003	.016 \pm .000
CLAD - ϵ -fair	.924 \pm .012	<u>.006</u> \pm .002	.406 \pm .027	.030 \pm .010	.716 \pm .004	.016 \pm .001
GSS - ϵ -fair	.938 \pm .006	<u>.006</u> \pm .002	.382 \pm .014	.035 \pm .017	.717 \pm .005	.016 \pm .000
OCS - ϵ -fair	<u>.952</u> \pm .003	.032 \pm .004	.384 \pm .009	.051 \pm .002	-	-
FSW - ϵ-fair	.906 \pm .006	.005 \pm .001	.405 \pm .013	.021 \pm .004	.723 \pm .004	.016 \pm .000

Table 19: Accuracy and fairness results on the MNIST and FMNIST datasets with respect to EER disparity. “FSW (hinge)” uses hinge loss, while “FSW” uses cross-entropy loss to approximate the group fairness metric.

Methods	MNIST		FMNIST	
	Acc.	EER Disp.	Acc.	EER Disp.
FSW	.925 \pm .004	.032 \pm .005	.824 \pm .006	.039 \pm .006
FSW (hinge)	.925 \pm .003	.030 \pm .006	.825 \pm .006	.039 \pm .005

Table 20: Accuracy and fairness results on the Biased MNIST, DRUG, and BiasBios datasets with respect to EO disparity. The other settings are the same as in Table 19.

Methods	Biased MNIST		DRUG		BiasBios	
	Acc.	EO Disp.	Acc.	EO Disp.	Acc.	EO Disp.
FSW	.909 \pm .004	.119 \pm .007	.406 \pm .014	.077 \pm .010	.808 \pm .002	.072 \pm .001
FSW (hinge)	.909 \pm .004	.119 \pm .006	.406 \pm .014	.077 \pm .010	.807 \pm .002	.071 \pm .002

Table 21: Accuracy and fairness results on the Biased MNIST, DRUG, and BiasBios datasets with respect to DP disparity. The other settings are the same as in Table 19.

Methods	Biased MNIST		DRUG		BiasBios	
	Acc.	DP Disp.	Acc.	DP Disp.	Acc.	DP Disp.
FSW	.904 \pm .004	.008 \pm .001	.405 \pm .013	.043 \pm .004	.809 \pm .003	.022 \pm .000
FSW (hinge)	.904 \pm .004	.008 \pm .001	.405 \pm .013	.043 \pm .004	.807 \pm .006	.022 \pm .000

B.15 Fairness Considerations in Buffering Strategy

Continuing from Sec. 3.3, we further elaborate on the distinct roles of buffering and sample weighting in our framework. Buffering primarily aims to preserve representative and diverse samples from previously learned groups, whereas sample weighting explicitly addresses the mitigation of unfair catastrophic forgetting during model training. Selecting buffer samples based on high fairness weights—those considered important for current-task fairness—might initially appear beneficial; however, this approach could inadvertently distort the original distribution of groups within the buffer. Modified distributions might negatively impact classification performance and complicate the accurate determination of fairness weights in future tasks. This complication arises because the buffer acts as a reference point for evaluating both fairness and accuracy metrics. Consequently, to maintain representative distributions and ensure reliable fairness measurement across tasks, we utilize a simple random sampling technique for buffer sample selection. For a fair comparison, we apply the same buffer usage across other baselines, without altering each method’s original buffer selection rule (e.g., herding or gradient-based selection).

To empirically validate this reasoning, we compare several buffering strategies, including random sampling (the original FSW) and sampling with a large-weight-first strategy. The results are shown in Tables 22, 23, and 24. Although the large-weight-first sampling strategy achieves comparable fairness results, the original random sampling method generally achieves superior accuracy, aligning with our theoretical expectations, while providing comparable or improved fairness performance.

Table 22: Accuracy and fairness results on the MNIST and FMNIST datasets with respect to EER disparity. “FSW (large-weight-first)” denotes a buffering strategy prioritizing samples with large weights, while “FSW” uses simple random sampling.

Methods	MNIST		FMNIST	
	Acc.	EER Disp.	Acc.	EER Disp.
FSW	.925±.004	.032±.005	.824±.006	.039±.006
FSW (large-weight-first)	.927±.005	.030±.003	.827±.005	.041±.008

Table 23: Accuracy and fairness results on the Biased MNIST, DRUG, and BiasBios datasets with respect to EO disparity. The other settings are the same as in Table 22.

Methods	Biased MNIST		DRUG		BiasBios	
	Acc.	EO Disp.	Acc.	EO Disp.	Acc.	EO Disp.
FSW	.909±.004	.119±.007	.406±.014	.077±.010	.808±.002	.072±.001
FSW (large-weight-first)	.893±.006	.124±.005	.405±.012	.077±.007	.800±.005	.071±.001

Table 24: Accuracy and fairness results on the Biased MNIST, DRUG, and BiasBios datasets with respect to DP disparity. The other settings are the same as in Table 22.

Methods	Biased MNIST		DRUG		BiasBios	
	Acc.	DP Disp.	Acc.	DP Disp.	Acc.	DP Disp.
FSW	.904±.004	.008±.001	.405±.013	.043±.004	.809±.003	.022±.000
FSW (large-weight-first)	.876±.009	.008±.001	.404±.013	.041±.005	.787±.014	.022±.001

B.16 Utilizing the Gradients of the Model’s Last Layer

Continuing from Sec. 3.3, we utilize the gradients of the model’s last layer during computation of the gradient vectors. Although using only the gradients from the model’s last layer may result in the loss of information from earlier layers, it significantly improves computational efficiency by reducing the gradient calculation time. This approach is theoretically supported by several studies [9, 44, 67]. Neglecting earlier layers is equivalent to substituting the gradient of model parameters in $\nabla_{\theta} \ell(f_{\theta}^{l-1}, d_i)$ of Eq. 1 to zero when the model parameter θ does not belong to the last layer. This simplification aligns with the statements from the references, “the variation of the gradient norm is mostly captured by the gradient of the loss function with respect to the pre-activation outputs of the last layer,” which implies that the last layer parameters dominate gradient contributions, making the parameters from earlier layers ignorable. Several studies [47, 48, 50] also only utilize the last layer’s gradients for efficiency.

To observe the efficiency of utilizing the last layer’s gradient, we conduct experiments comparing the performance and runtime between utilizing the full gradient and the last layer’s gradient, as shown in Table 25. Using only the last layer’s gradients provides comparable accuracy and fairness to using gradients from all layers, while significantly reducing the gradient computation time. The CPLEX computation time is comparable since the number of variables and constraints remains unchanged. In addition, the model training time increases when using gradients from all layers, primarily due to an increase in the average number of non-zero sample weights (from 2863.4 to 4280.5), resulting in a higher number of batches during training.

Table 25: Accuracy, fairness, and runtime results on the Biased MNIST datasets with respect to EO disparity. “FSW” utilizes gradients of the model’s last layer during computation of the gradient vectors, while “FSW (all layers)” utilizes gradients of all model parameters during computation.

Methods	Acc.	EO Disp.	Gradient Computation	CPLEX Computation	Model Training
FSW	.909±.004	.119±.007	233±017 (s)	507±004 (s)	94±003 (s)
FSW (all layers)	.910±.005	.117±.009	23,843±882 (s)	578±003 (s)	184±010 (s)

B.17 Alternative Optimization Solver for Linear Programming

Continuing from Sec. 4.1, we conduct experiments comparing CPLEX with another optimization solver, HiGHS [40]. Tables 26, 27, and 28 show accuracy and fairness on FSW with CPLEX and HiGHS solver with respect to EER, EO, and DP disparity. We observed that both solvers show comparable accuracy-fairness results, suggesting that FSW is robust to the choice of LP solver in practice. While other solvers can be used, we use CPLEX in our paper due to its strong solution stability and high speed in solving large-scale problems with numerous variables and constraints. CPLEX also provides comprehensive tools for in-depth solution analysis, and is thus widely used in the literature [36, 79, 94].

Table 26: Accuracy and fairness results on the MNIST and FMNIST datasets with respect to EER disparity. “FSW (using CPLEX)” uses CPLEX as an optimization solver, while “FSW (using HiGHS)” uses HiGHS as an optimization solver.

Methods	MNIST		FMNIST	
	Acc.	EER Disp.	Acc.	EER Disp.
FSW (using CPLEX)	.925±.004	.032±.005	.824±.006	.039±.006
FSW (using HiGHS)	.925±.004	.031±.006	.825±.006	.039±.007

Table 27: Accuracy and fairness results on the Biased MNIST, DRUG, and BiasBios datasets with respect to EO disparity. The other settings are the same as in Table 26.

Methods	Biased MNIST		DRUG		BiasBios	
	Acc.	EO Disp.	Acc.	EO Disp.	Acc.	EO Disp.
FSW (using CPLEX)	.909 \pm .004	.119 \pm .007	.406 \pm .014	.077 \pm .010	.808 \pm .002	.072 \pm .001
FSW (using HiGHS)	.907 \pm .005	.117 \pm .006	.406 \pm .014	.077 \pm .010	.805 \pm .004	.070 \pm .002

Table 28: Accuracy and fairness results on the Biased MNIST, DRUG, and BiasBios datasets with respect to DP disparity. The other settings are the same as in Table 26.

Methods	Biased MNIST		DRUG		BiasBios	
	Acc.	DP Disp.	Acc.	DP Disp.	Acc.	DP Disp.
FSW (using CPLEX)	.904 \pm .004	.008 \pm .001	.405 \pm .013	.043 \pm .004	.809 \pm .003	.022 \pm .000
FSW (using HiGHS)	.902 \pm .006	.009 \pm .002	.405 \pm .013	.043 \pm .004	.807 \pm .004	.022 \pm .000

C More Related Work

Continuing from Sec. 2, we discuss more related work.

Class-incremental learning is a challenging type of continual learning where a model continuously learns new tasks, each composed of new disjoint classes, and the goal is to minimize catastrophic forgetting [60, 61]. Data replay techniques [20, 58, 73] store a small portion of previous data in a buffer to utilize for training and are widely used with other techniques [96] including knowledge distillation [14, 73], model rectification [86, 95], and dynamic networks [84, 91, 97]. Simple buffer sample selection methods such as random or herding-based approaches [73] are also commonly used as well. There are also gradient-based sample selection techniques like GSS [4] and OCS [92] that manage buffer data to have samples with diverse and representative gradient vectors. The core contribution of FSW is its capability to separately address different groups through sample weighting, and all baseline works do not consider fairness and simply assume that the entire incoming data is used for model training, which may result in unfair forgetting, as we show in our experiments.

Model fairness research mitigates bias by ensuring that a model’s performance is equitable across different sensitive groups, thereby preventing discrimination based on race, gender, age, or other sensitive attributes [64]. Existing model fairness techniques can be categorized as pre-processing [15, 33, 41, 43], in-processing [2, 25, 74, 93], and post-processing [23, 38, 71]. In addition, there are other techniques that assign adaptive weights for samples to improve fairness [16, 42]. However, most of these techniques assume that the training data is given all at once, which may not be realistic. There are techniques for fairness-aware active learning [5, 68, 80], in which the training data evolves with the acquisition of samples. However, these techniques store all labeled data and use them for training, which is impractical in continual learning settings.

A recent study addresses model fairness in class-incremental learning, where models may suffer from imbalanced forgetting of previously learned sensitive groups including classes, leading to unfairness across different groups [21, 39, 81, 88] (see more details in

Sec. C). A recent study [39] addresses the dual imbalance problem involving both inter-task and intra-task imbalance by reweighting gradients. However, the bias arises not only from data imbalance, but also from inherent or acquired characteristics of data itself [7, 64]. CLAD [88] first discovers imbalanced forgetting between classes caused by conflicts in representation and proposes a class-aware disentanglement technique to improve accuracy. Among the fairness-aware techniques, FaRL [21] supports group fairness metrics like demographic parity for continual learning, but proposes a representation learning method that does not directly optimize the given fairness measure and thus has limitations in improving fairness as we show in experiments. FairCL [81] also addresses fairness in a continual learning setup, but only focuses on resolving the imbalanced class distribution based on the number of pixels of each class in an image for semantic segmentation tasks. In comparison, we can mitigate bias from both data imbalance and intrinsic or acquired characteristics within the data with satisfying multiple notions of group fairness for sensitive groups including classes.

D Future Work

Continuing from Sec. 5, we discuss the future work in more detail.

D.1 Generalization to Multiple sensitive attributes

FSW can be extended to tasks involving multiple sensitive attributes by defining a sensitive group as a combination of sensitive attributes. For instance, recall the loss for EO in a single sensitive attribute is $\frac{1}{|\mathbb{Y}||\mathbb{Z}|} \sum_{y \in \mathbb{Y}, z \in \mathbb{Z}} |\tilde{\ell}(f_{\theta}, G_{y,z}) - \tilde{\ell}(f_{\theta}, G_y)|$. This definition can be extended to the case of multiple sensitive attributes as $\frac{1}{|\mathbb{Y}||\mathbb{Z}_1||\mathbb{Z}_2|} \sum_{y \in \mathbb{Y}, z_1 \in \mathbb{Z}_1, z_2 \in \mathbb{Z}_2} |\tilde{\ell}(f_{\theta}, G_{y,z_1,z_2}) - \tilde{\ell}(f_{\theta}, G_y)|$. The new definition for multiple sensitive attributes allows the overall optimization problem to optimize both sensitive attributes simultaneously. The design above can also help prevent ‘fairness gerrymandering’ [46], a situation where fairness is superficially achieved across multiple groups, but specific individuals or subgroups within those groups are systematically disadvantaged. This is achieved by minimizing all combinations of subgroups, thereby disrupting the potential for unfair prediction based on certain attribute combinations. However, having multiple loss functions may increase the complexity of optimization, and a more advanced loss function may need to be designed for multiple sensitive attributes.

D.2 Further Reduction of Computational Overhead

The scalability of FSW can be further improved for large datasets, particularly when the quadratic computational complexity becomes a bottleneck. Continuing from Sec. B.3, clustering current data and assigning cluster-wise weight reduce LP variables, lowering computational complexity. Mini-batch K-means [77] is efficient for extremely large datasets where the complexity is $O(\text{BKDI})$ (B: batch size, K: number of clusters, D: data dimension, I: number of iterations).

Beyond clustering, another approach is reducing the complexity of LP using a first-order method, which results in a complexity of $O(\text{ND})$ (N: number of current task samples, D: data dimension).

CPLEX solves LP based on the simplex method [13], which is accurate, but computationally intensive due to Hessian calculations. First-order methods, by contrast, rely only on gradient information and thus offer better scalability for large datasets [11]. Moreover, these two approaches—clustering and first-order optimization—are orthogonal and can be combined to further improve FSW’s scalability on extremely large datasets.

D.3 Possible Strategies Under Data Drift

Data drift can be categorized into two types: virtual drift and concept drift [35]. Virtual drift refers to changes in the data distribution that do not alter the decision boundary. In such cases, model performance may slightly degrade, but FSW can eventually adapt to the

new distribution while preserving previously learned knowledge. This adaptation is possible because FSW adjusts weights based on gradients derived from both the data and the model, allowing it to maintain flexibility and resilience against mild distributional changes. On the other hand, concept drift occurs when the decision boundary shifts. In class-incremental learning, such shifts can be interpreted as the noise introduced into the true label (y) prior to the concept drift, thereby complicating the fairness maintenance. To address this, combining FSW with robust training methods that are effective under noisy label conditions could be a potential direction. This integration would enhance both fairness and robustness, ensuring the model’s performance despite shifts in the decision boundary.